



## Pacific-type transform and convergent margins: igneous rocks, geochemical contrasts and discriminant diagrams

Andrei V. Grebennikov & Alexander I. Khanchuk

To cite this article: Andrei V. Grebennikov & Alexander I. Khanchuk (2021) Pacific-type transform and convergent margins: igneous rocks, geochemical contrasts and discriminant diagrams, International Geology Review, 63:5, 601-629, DOI: [10.1080/00206814.2020.1848646](https://doi.org/10.1080/00206814.2020.1848646)

To link to this article: <https://doi.org/10.1080/00206814.2020.1848646>



View supplementary material [↗](#)



Published online: 09 Dec 2020.



Submit your article to this journal [↗](#)



Article views: 208



View related articles [↗](#)





View Crossmark data [↗](#)

REVIEW ARTICLE



## Pacific-type transform and convergent margins: igneous rocks, geochemical contrasts and discriminant diagrams

Andrei V. Grebennikov  and Alexander I. Khanchuk 

Far Eastern Branch, Russian Academy of Sciences, Far East Geological Institute, pr. 100-letiya Vladivostoku 159, Vladivostok, 690022 Russia

### ABSTRACT

Transform margins represent lithospheric plate boundaries with horizontal sliding of the oceanic plate, which in time and space replaced the subduction-related convergent margins. This happened due to the following: ridge-crest–trench intersection or ridge death along a continental margin (recent California and Baja California, Queen Charlotte–Northern Cordilleran, west of the Antarctic Peninsula, and probably Late Miocene–Pleistocene southernmost South America); change in the direction of oceanic plate movement (western Aleutian–Komandorsk and southernmost tip of the Andes); and island arc–continent collision (New Guinea Island). Post-subduction magmatism is related to a slab window that resulted from the spreading ridge collision (subduction) with a continental margin or slab tear formation after subduction cessation. Igneous magmatic series formed above the slab window or slab tear are similar in composition and show diversity of tholeiitic (sub-alkaline), alkaline, or even calc-alkaline and peraluminous rocks. The comprehensive geochemical dataset for igneous rocks (more than 2400 analyses) from the recent model geodynamic settings allowed us to build discriminant diagrams for the petrogenic oxides  $\text{TiO}_2 \times 10 - \text{Fe}_2\text{O}_3^{\text{Tot}} - \text{MgO}$  and trace elements  $\text{Nb}^*5 - \text{Ba}/\text{La} - \text{Yb}^*10$ , which show distinctive rock features present on both convergent and Pacific-type transform margins. The author's diagrams are capable of distinguishing volcanic and plutonic rocks formed above the subduction zones at an island arc and continental margin (related to convergent margins), from those formed in the strike-slip tectonic setting of transform margins along continents or island arcs.

### ARTICLE HISTORY

Received 10 November 2019  
Accepted 7 November 2020

### KEYWORDS

Tectonic settings; slab tear; slab window; subslab asthenosphere; adakite; geochemistry; discriminant diagrams

## Introduction

An important problem of modern geology is in trying to accurately use geochemical datasets and identifying criteria of magmatism at various Pacific-type margins to infer a geodynamic/tectonic setting. This can be used for plate reconstructions in ancient time since it is increasingly often reconstructed as a combination of convergent and transform geodynamic settings alternating in both time and space (e.g., Natal'in 1993; Sengör and Natal'in 1996; Khanchuk and Ivanov 1999; Patchett and Chase 2002; Grebennikov 2014; Shen *et al.* 2014; Grebennikov *et al.* 2016; Khanchuk *et al.* 2016, 2019; Martynov *et al.* 2017).

Transform and convergent margins represent different types of transition zones between oceanic and continental or island arc lithosphere. A convergent margin is an area where oceanic lithosphere is subducted into the mantle beneath a continent or island arc. The concept of transform margins came from the definition of transform faults as a 'new class of faults', where a lithospheric plate boundary is parallel to the

relative plate displacement and two plates slide horizontally past one another (Wilson 1965). Atlantic and Pacific types of transform margins can be distinguished. The first type occurs at the extensions of previously active transform faults that earlier crossed passive margins, while the Pacific-type transform margins are extensions of active (convergent) margins (e.g., Basile 2015; de Lépinay *et al.* 2016).

There are three major tectonic settings of the Pacific-type transform and convergent margin transit resulting from a ridge-crest–trench intersection or ridge death along a continental margin; change in the direction of oceanic plate movement; and island arc–continent collision.

Magmatism at transform margins following ridge-crest–trench intersection is interpreted as caused by asthenospheric upwelling and adiabatic decompression as a result of the formation of a slab window (Dickinson and Snyder 1979a; Thorkelson and Taylor 1989; Hole *et al.* 1991; Liu and Furlong 1992; Thorkelson 1996; Gorrington and Kay 2001; Breitsprecher and Thorkelson

2009; Groome and Thorkelson 2009; Guenther *et al.* 2010; Guillaume *et al.* 2013).

The first study of convergent-transform plate boundary transit was performed in California. The San Andreas transform was initiated locally when a segment of the ancestral East Pacific rise first encountered the subduction zone along the continental margin. The resulting Pacific-American transform has since gradually lengthened by the simultaneous northward and southward migration of the two triple junctions that define the ends of the transform plate boundary (Atwater 1970; Dickinson and Snyder 1979a). Dickinson and Snyder (1979b) recognized that generation of a lengthening transform by a rise-trench encounter will also generate an expanding triangular hole or window in the slab of lithosphere subducted beneath the continent.

In a landmark paper, Thorkelson (1996) developed the geometrical models of slab-window formation depending on the angle of ridge-crest-trench intersections. *'In these situations, commonly referred to as "ridge subduction", the newly formed trailing edge of one or both of the diverging oceanic plates descends into the asthenosphere'*. One of these models explains the formation of a transform margin by low-angle convergence of a highly segmented ridge (Thorkelson 1996). West of the Baja California transform margin, however, the remnants of the Pacific-Farallon fossil ridge ceased approximately 12.5 Ma have been identified (e.g., Batiza 1977; Lonsdale 1991; Wilson *et al.* 2005), and close to it there is the fossil trench reflecting the former California subduction zone where the Farallon plate was being subducted until 13 Ma (Atwater 1970). This indicates that active ridge subduction was not responsible for the opening of the asthenospheric window beneath Baja California and east of it. To explain this fact, namely ridge-trench collision and ridge death, several models of opening of a trench-parallel slab gap, tear or window within the stalled slab of the Farallon plate were proposed by different authors (e.g., Dickinson 1997; Michaud *et al.* 2006; Pallares *et al.* 2007; Castillo 2008; Calmus *et al.* 2011; Negrete-Aranda *et al.* 2013; Di Luccio *et al.* 2014, and references therein).

The most popular understanding of the slab-window term implies just subduction of a spreading-ridge and nothing more (McCrory and Wilson 2009; Eyuboglu 2013; Windley and Xiao 2018, and references therein). When the formation of a window in a slab on a transform margin is not related to a spreading-ridge subduction, the terms slab tear, slab gap, slab broke, and slab break-off are used (e.g., Guivel *et al.* 2006; Pallares *et al.* 2007; Castillo 2008; Breitsprecher and Thorkelson 2009; Georgieva *et al.* 2019). Some authors, however, still used the term 'slab window' for a slab gap on a transform margin not related to a spreading-ridge

subduction (e.g., Michaud *et al.* 2006; Negrete-Aranda *et al.* 2013; Mark *et al.* 2017). It is noteworthy that a slab window could form in a setting not transform margin-related, such as orthogonal spreading-ridge subduction (e.g., Kinoshita 1999; Windley and Xiao 2018, and references therein), while a slab tear, slab gap, slab break-off, slab failure, etc., are supposed to be formed in an arc-continent collision and collisional orogeny, for example (e.g., Davies and von Blanckenburg 1995; Keskin 2003, 2007; Cloos *et al.* 2005; Garzanti *et al.* 2018; Whalen and Hildebrand 2019). A slab tear can form at the extension of a transform fault under a continental margin, e.g., the Nootka fault separates the subducted slabs of the Explorer and Juan de Fuca plates underneath the interior areas of British Columbia and forms a slab tear (Madsen *et al.* 2006). Slab window or slab tear formation is described as a result of orthogonal collision-subduction of the aseismic Cocos ridge beneath the Central American arc (Abratis and Wörner 2001).

In future discussions, the term 'slab window' will be used only for the settings related to subduction of mid-ocean ridge, while in other cases the term 'slab tear' will be used. Slab-window forms at the ocean-continent boundary and slab tear is located in some distance from the ocean-continent boundary, and between this boundary and slab tear a slab fragment is identified according to the geophysical data. A more detailed information on this is in the 'California and Baja California' section.

Convergent-transform margin transit related to changes in the direction of oceanic plate movement is conditioned by reorganization of the Pacific plate's movement (e.g., Engebretson *et al.* 1985). Tectonic reconstructions of the Pacific arc-continent collision usually do not discuss the character of the zone between the continent, accreting arc, and oceanic plate after subduction termination. The example of New Guinea shows that this zone was evidently not a passive margin, as the Pacific plates kept moving and the boundary between the continental margin and oceanic plate was the boundary of sliding before a new subduction zone formed (e.g., Cloos *et al.* 2005).

Convergent margins are characterized by the subduction of a cold oceanic lithosphere into a hot convective mantle. The lines of evidence for a convergent (subduction-related) magmatic origin are now numerous. However, the magmatism does not always accompany convergence/subduction (McCarthy *et al.* 2020, and references therein). Key trace element ratios (Ba/Nb – total subduction component; Th/Ta, and Th/Nb – deep subduction component; Ba/Ta, and Ba/Th – shallow subduction component, etc.) based on geochemical fingerprinting versus tectonic setting provided the

petrogenetic insights, and attempts to isolate the different subduction components were performed (e.g., Pearce *et al.* 2005; Pearce and Robinson 2010; Pearce 2014).

The magmatic rock geochemistry of transform margins is based on investigations of modern and late Cenozoic settings of a slab window or a slab tear and depends on the subslab asthenosphere displaying enriched (OIB) or depleted mantle (MORB) signatures (e.g., Thorkelson and Taylor 1989; Sharma *et al.* 1991; Cole and Basu 1995; Hole *et al.* 1995; Thorkelson 1996; Gorrington *et al.* 1997; Gorrington and Kay 2001; Weigand *et al.* 2002; Groome *et al.* 2003; Keskin 2003, 2007; Pallares *et al.* 2007; Castillo 2008; Ickert *et al.* 2009; Kant *et al.* 2018). A number of binary diagrams have been proposed for discriminating these sources in different Late Cenozoic geodynamic settings (not only in transform margins). Abratis and Wörner (2001) used Nb/Zr and Ba/La ratios as crucial parameters to characterize the enrichment and depletion of mantle magma sources related to the subduction of the aseismic Cocos Ridge beneath the Central American arc and the subsequent opening of a slab window. These authors showed that high Ba/La and low Nb/Zr ratios of the rocks before 8 Ma suggest derivation from a fluid-modified, depleted-mantle wedge, which is typical of 'normal' arc magmatism. At the same time, alkalic volcanic and intrusive rocks between 5.8 and 2 Ma have low Ba/La ratios and high Nb/Zr ratios that indicate derivation from partial melting of enriched-mantle material typical of an OIB source. An investigation of Miocene–Holocene volcanoes along a 3500-km-long transect from the northern Cascade Arc to the Aleutian Arc across the Northern Cordilleran slab-window or Queen Charlotte–Northern Cordilleran transform margin was performed using geochemical Nb/Zr and La/Nb ratios, and the results showed that typical volcanic arc compositions in the Cascade and Aleutian systems are separated by an extensive transform margin volcanic field with intraplate compositions and higher Nb/Zr values (Thorkelson *et al.* 2011).

Keskin (2003, 2007) used the Th/Ta ratio of basic samples (with MgO > 3 wt% and SiO<sub>2</sub> < 52 wt%) for Late-Miocene–Recent volcanic rocks of Eastern Anatolia. This ratio is independent of partial melting and fractional crystallization and can be used to differentiate between lavas with subduction and intraplate signatures. He pointed out that lavas containing a distinct subduction signature have consistently higher Th/Ta ratios and, in general, lower Ta concentrations compared to post-collisional slab break-off related lavas.

Pearce (2014) indicated that Ti/Yb is only high in products of deep melting where garnet is stable. Thus, Ti/Yb versus Nb/Yb may be used to differentiate ocean

island basalts (deep melting and high Ti/Yb) from MORB (shallow melting and low Ti/Yb).

The earlier proposed binary discriminant diagrams were better able to identify non-subductional alkali mafic rocks with intraplate signature compared with other rocks. In Late Cenozoic margins of Pacific rim calc-alkaline mafic, intermediate and felsic rocks, and high-Mg# volcanic rocks with adakitic affinity are present on both convergent and transform margins. However, their geochemical differences have not been studied due to their complexity. One of the principal obstacles in tectonic reconstructions consists of the absence of fields for transform margin magmatism on current geochemical discrimination plots.

The authors made an attempt to fill this gap by a comparative geochemical analysis of different geodynamic convergent and transform margins in the Pacific region (Figure 1) and to propose discriminant diagrams capable of reliably distinguishing the supra-subduction island arc and continental margin types of magmatism (related to convergent margins) and the transform sliding of lithospheric plates at ocean margins (related to transform margins).

### Geodynamics and magmatism of the Pacific-type transform margins

Several examples of transform margins may be found along the Pacific rim, which formed as follows: 1) resulting from a ridge-crest–trench intersection or ridge death along a continental margin (California and Baja California, Queen Charlotte–Northern Cordilleran, Antarctic Peninsula, and probably the Late Miocene–Pleistocene margin of southernmost South America); 2) change in the direction of oceanic plate movement (west Aleutian–Komandorsk and southernmost tip of the Andes); and 3) island arc-continent collision (New Guinea Island).

#### Transform margins related to a ridge-crest–trench intersection or ridge death along a continental margin

##### California and Baja California

These geodynamic settings are best studied in western North America in California and Baja California, where the Pacific and North American plates slide past each other horizontally and where the latest Cenozoic magmatism related to strike-slip tectonics occurs from the Pacific coast to the Basin and Range province (Figure 2). Dickinson and Snyder (1979a), considering earlier works (McKenzie and Morgan 1969; Atwater 1970), laid the foundation for the modern ideas about the formation



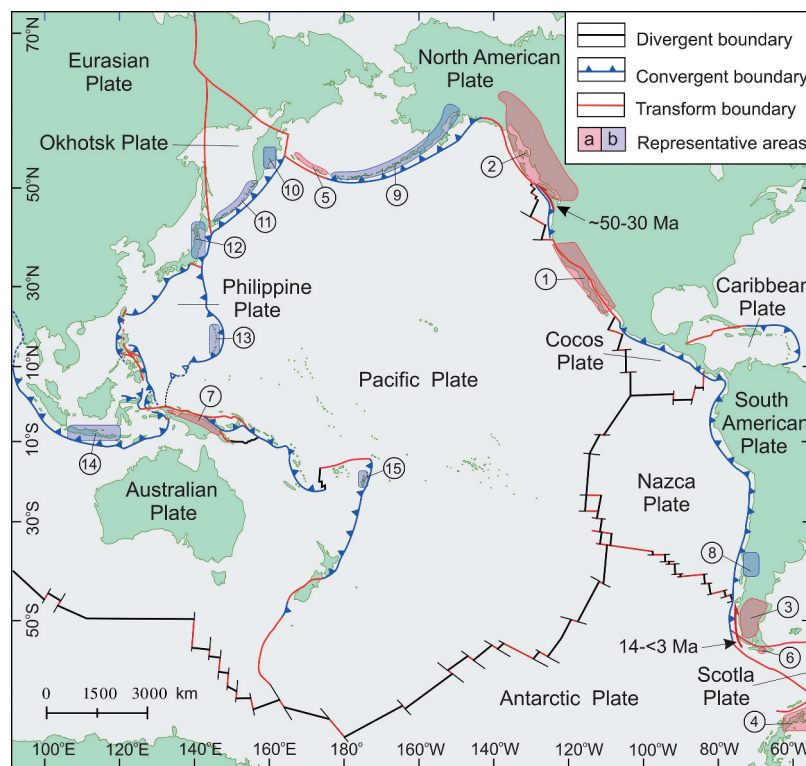


**Figure 1.** The representative areas of Pacific-type transform and convergent margins: 1) California and Baja California; 2) Queen Charlotte–Northern Cordilleran; 3) Southernmost South America; 4) West of the Antarctic Peninsula; 5) Western Aleutian–Komandorsk; 6) Southernmost tip of the Andes; 7) New Guinea Island; 8) Central South Volcanic Zone of the Andes, 37°S–41.5°S; 9) Aleutian Islands, Alaska to Buldir Island; 10) Eastern Kamchatka; 11) Kuril arc; 12) NE Japan; 13) Southern Pagan Island lavas, Mariana arc; 14) Java–Sunda arc; and 15) Tonga arc and submarine Monowai volcanic centre, northern Kermadec arc, SW Pacific. Red arrow indicates the fossil transform margin. (a) – Transform margins; (b) – Convergent margins.

and evolution of the transform plate boundary. According to the proposed model, the transform plate boundary began to form after ridge-crest-trench intersection, leading to a change in the direction of motion of the Pacific plate, causing slab breaks at some points as well as the formation of an area with no slab beneath the continent or a 'slab window'. This slab window continued to grow as the Mendocino and Rivera triple junctions migrated north and south, respectively (Dickinson and Snyder 1979b). Severinghaus and Atwater (1990) argued that instead of a slab window developing from west to east, a slab gap developed from the east and then propagated north and south with the Mendocino and Rivera triple junctions. Overall, the slab gap is only a modified version of the slab window, and both can be used to explain the cessation of arc volcanism.

However, magnetic anomalies on the Pacific plate and tectonic reconstructions have shown that the San Andreas transform fault system originated at approximately 27 Ma in response to collision between the East Pacific rise and the former Farallon–North America subduction zone. The collision process was accompanied by fragmentation of the Farallon plate into several

microplates, including the Monterey (27–19 Ma), Arguello (20–18 Ma), Guadalupe (20–14 Ma), Magdalena (14–12 Ma) and Rivera plates (5 Ma–present). The Arguello-Pacific and most of Monterey-Pacific ridges subducted and caused the formation of a slab window beneath California, in which hot asthenospheric mantle wells up in the gap created between the two diverging plates (e.g., Dickinson 1997; McCrory *et al.* 2009) (Figure 3A). A small unsubducted fragment of the Monterey plate has been revealed in California near the coastline and slab tear beneath the continental margin (Wilson *et al.* 2005; Wang *et al.* 2013).

West of Baja California, Guadalupe and Magdalena microplates ceased subducting before the spreading centre reached the trench and was captured by the Pacific plate stagnant slabs attached to them, extending into the mantle as deep as 200 km (Wang *et al.* 2013). Baja California rifted apart from the Mexico mainland along the dextral strike-slip fault subparallel to the continental margin. The partially subducted Guadalupe and Magdalena microplates reversed direction and began to move with the Pacific plate away from coastal Mexico. Landward propagation of the plate boundary was

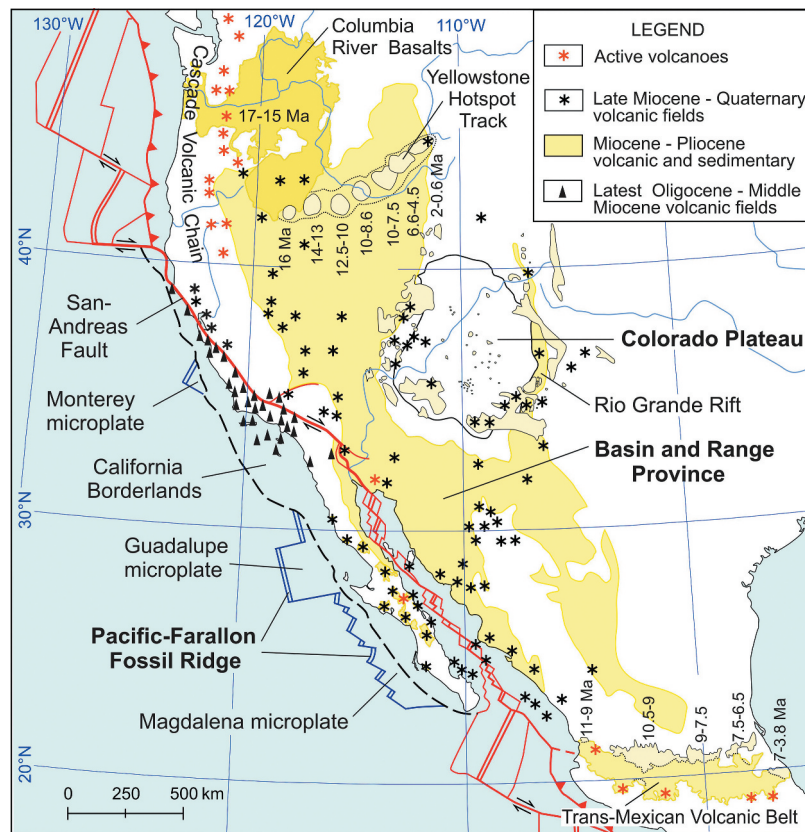


**Figure 2.** Late Cenozoic geodynamics and magmatic complexes of California and Baja California as a result ridge-crest–trench intersection or ridge death along a continental margin (tectonic base after Dickinson 2002; McCrory *et al.* 2009); magmatic complexes after Sahagian *et al.* 2002; Weigand *et al.* 2002; Ferrari 2004; Castillo 2008; Sweetkind *et al.* 2011; Bryan *et al.* 2014; Valentine *et al.* 2017).

accompanied by a discrete ‘jump’ of the major fault in the system. The present-day Pacific–North America plate boundary is located mostly in the continent, rather than offshore (Stock and Hodges 1989; Lonsdale 1991; Dickinson 1997; Wilson *et al.* 2005; McCrory and Wilson 2009; Mark *et al.* 2017, and references therein).

Thus, the microplate capture model, also known as the ‘stalled slab’ concept (Bohannon and Parsons 1995) provides a direct and effective mechanism for transferring North American continental crust to the Pacific plate. This model argues that more regional upwelling of Pacific asthenosphere occurred when the slab broke off beneath the proto-Gulf of California once the spreading ridge died near the trench and the subduction of the Guadalupe and Magdalena microplates ceased. Injected through a newly formed slab tear, the slab asthenosphere provided a mantle source for post-subduction magmas, which eventually led to the formation of the Gulf of California rift zone (Michaud *et al.* 2006; Pallares *et al.* 2007; Castillo 2008; Negrete-Aranda *et al.* 2013) (Figure 3B).

Latest Oligocene to Middle Miocene post-subduction volcanism in western and offshore California occurred

during the transition from convergent to transform plate boundaries as segments of the East Pacific rise intersected a subduction zone (see Figure 2). The southwestern side of the San Andreas fault system (on both sides in the area of the Garlock fault) implies progressively younger volcanic emplacement to the southeast from ~25 Ma (~39°N) to 12.5 Ma (~34°N) according to consequent ridge-crest–trench intersections (Dickinson 1997; Weigand *et al.* 2002; McCrory *et al.* 2009; Day *et al.* 2019). The latest Miocene (~5.5 Ma) to Quaternary (~0.9 Ma) magmatic rocks of the north-eastern side of the San Andreas fault system become younger in the north-western direction (e.g., linear belt of volcanic fields north of San Francisco Bay). This is associated with the north-western migration of the Mendocino triple junction (Sweetkind *et al.* 2011).

Ridge-crest–trench intersection volcanism in California is represented by basalt, basaltic andesite, dacite, and rhyolite that erupted closely spaced in time in both submarine and subaerial conditions. These rocks belong to the calc-alkaline magma series and are characterized by low K<sub>2</sub>O contents. The petrogenesis of the basalts is explained by the involvement of

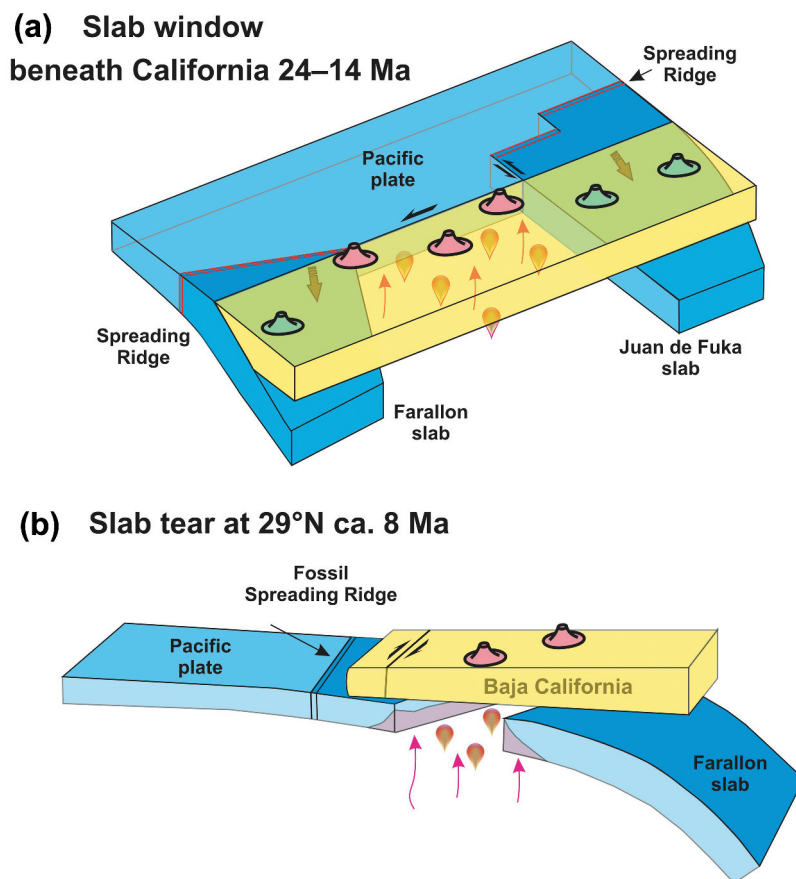


**Figure 3.** Compilation models for the slab window (A) after McCrory *et al.* 2009, and slab-tear (B) after Pallares *et al.* 2007.

subcontinental lithosphere, depleted upper mantle source similar to MORB and local continental crust (e.g., Sharma *et al.* 1991). The generation of rhyolitic melts due to crustal assimilation by basaltic melts was produced by the assimilation of variable amounts of continental crust by MORB-related magmas and subcontinental lithosphere-derived melts (Sharma *et al.* 1991; Cole and Basu 1995; Weigand *et al.* 2002).

The consequent evolution of slab window-related volcanism, for example, north of San Francisco Bay, is represented by Pliocene–Quaternary basalt, basaltic andesite, andesite, and rhyolite (Schmitt *et al.* 2006; Sweetkind *et al.* 2011). Volcanic centres are characterized by the following individual compositions: 1) from mafic to silicic; 2) from dominantly basaltic to andesitic; and 3) dominantly silicic volcanic. Mafic rocks of the Sonoma and Clear Lake volcanic fields generally have medium-K calcalkaline series compositions, with generally increasing total alkali contents with silica and are clearly distinguished from rocks of the ancestral and modern Cascades magmatic arc in having elevated  $\text{TiO}_2$  concentrations and low LILE/HFSE ratios (Sweetkind *et al.* 2011). The volcanism of the south side of Garlock fault in the Lava Mountains is similar to the volcanism north of San

Francisco Bay that occurred between 11.7 and 5.8 Ma (Smith *et al.* 2002).

In the east, California slab-window volcanism extends to the Basin and Range province. In the Mojave Desert, since at least 8 Ma, most of the basalts were derived from asthenosphere isotopically identical to the source of Pacific MORB in response to the passive upwelling of asthenospheric mantle into a slab gap that developed in this region during the initiation of the San Andreas transform fault system (Farmer *et al.* 1995). In the Death Valley area, there are the latest Miocene to middle Pliocene rocks from basalt to dacite with dominant basaltic andesite and very rare high-silica units. Their chemical and isotopic characteristics record interaction of the ancient crust, enriched and lithosphere mantle. This is consistent with extension across the southern Basin and Range province inferred from other evidence (Coleman and Walker 1990).

Late Miocene to Quaternary igneous rocks of Baja California related to the ridge death and slab tear along the continental margin are characterized by exceptional geochemical diversity (e.g., Gastil *et al.* 1979; Benoit *et al.* 2002). On the whole, mafic lavas represent a number of basaltic compositions from

depleted MORB to alkalic peralkaline basalts along with their intermediate variations and, less frequently, with Nb-enriched basalts (Aguillón-Robles *et al.* 2001). More siliceous variations include unusual rocks such as icelandites and peraluminous A-type rhyolites (Vidal-Solano *et al.* 2008), magnesian andesites (Saunders *et al.* 1987; Calmus *et al.* 2003) and adakites (Aguillón-Robles *et al.* 2001; Calmus *et al.* 2008). The curious association of adakites with alkaline rocks enriched in HFSEs and Cu-Au mineral deposits as well as diagnostic chemical characteristics of adakites have permitted a number of authors to infer that these rocks form in unique tectonic settings where the subducting slab is abnormally heated and melts as a result of breaking of the slab, leading to the opening of asthenospheric windows or slab tear (e.g., Yogodzinski *et al.* 2001; Calmus *et al.* 2003; Gao *et al.* 2007; Castillo Castillo, P.R., 2012). Volcanic rocks related to the transform margin in the southern Basin and Range are represented by Late Miocene (12 Ma) and Pliocene hawaiite as well as Quaternary basalt (Henry and Aranda-Gomez 2000).

### **Queen Charlotte–northern Cordilleran**

The Queen Charlotte fault forms one of Earth's great transform margins and extends from southern British Columbia to Alaska. The dextral-slip Queen Charlotte fault systems are the result of the Pacific plate moving north-west along the margin of the North American plate. They extend from the Explorer triple junction north of Vancouver Island to the eastern end of the Chugach-St. Elias mountain range, a distance of 1,200 km (Walton *et al.* 2015; Ten Brink *et al.* 2018). The Queen Charlotte transform margin began at  $\sim$ 53 Ma after ridge-crest–trench intersection of the Kula-Resurrection or Kula-Resurrection and Eshamy ridges subparallel to a continental margin from the area south of the modern Vancouver Island to Alaska (Haeussler *et al.* 2003; Madsen *et al.* 2006). At  $\sim$ 40 Ma, the Kula and Eshamy plates became fused to the Pacific plate. The Pacific plate began to move in approximately transform motion with respect to the Queen Charlotte transform fault system (Madsen *et al.* 2006).

In forearc, the subduction of a spreading centre parallel to a continental margin and formation of a slab window produces diverse Eocene mafic and felsic magmatism occurring in Alaska, the Queen Charlotte (Haida Gwaii) Islands, Vancouver Island, and Oregon area (e.g., Babcock *et al.* 1992; Breitsprecher *et al.* 2003; Haeussler *et al.* 2003; Madsen *et al.* 2006). Voluminous tholeiitic basalts resemble MORB, and calc-alkaline basaltic andesites are enriched in LREE but are not strongly depleted in Nb. The rocks have overlapping isotopic compositions, similar to those of intraplate basalts (Hamilton

and Dostal 2001). Eocene tonalite-trondhjemite and bimodal suites are interpreted to be products of forearc melts mixed with mid-ocean-ridge basalt magmas during ridge–trench interaction (Groome *et al.* 2003). In back-arc, adakitic volcanism formed simultaneously with the beginning of (53–47 Ma) forearc ridge-crest–trench intersection. The formation of adakites has been caused by upwelling asthenosphere related to a slab tear (Ickert *et al.* 2009). The Eocene Challis-Kamloops volcanic belt that extends from Yukon across British Columbia to the northern United States was running approximately parallel to the Queen Charlotte fault. This belt is composed of high-K calc-alkaline mafic and intermediate lavas and is probably related to a slab window formation (Dostal *et al.* 2001; Breitsprecher *et al.* 2003).

Recently, the northern Cordilleran volcanic province related to the Queen Charlotte transform margin encompasses a broad area of Neogene to Quaternary volcanism in western British Columbia, the Yukon Territory, and adjacent eastern Alaska. Volcanic rocks of the northern Cordilleran volcanic province range in age from 20 Ma to ca. 200 yr B.P. and are dominantly alkali olivine basalt and hawaiite. A variety of more strongly alkaline rock types not commonly found in the North American Cordillera are locally abundant in the northern Cordilleran volcanic province. These include nephelinite, basanite, and peralkaline phonolite, trachyte, and comendite. They show trace element abundances and isotopic compositions that are consistent with an asthenospheric source region similar to that for average oceanic island basalt and for post-5 Ma alkaline basalts from the Basin and Range (Edwards and Russell 2000). A database of 3530 analyses from Miocene–Holocene volcanoes along a 3500-km-long transect, from the northern Cascade Arc to the Aleutian Arc, was used to show that typical volcanic arc compositions in the Cascade and Aleutian systems (derived from subduction-hydrated mantle) are separated by an extensive volcanic field with intraplate compositions (derived from relatively anhydrous mantle) (Thorkelson *et al.* 2011). The transition from subduction to a right-lateral translation north ridge crest–trench intersection may have created post-subduction Cenozoic magmatism within the former forearc and accretionary prism is explained by the existence of a slab window under the margin (Thorkelson and Taylor 1989; Edwards and Russell 2000; Haeussler *et al.* 2003; Madsen *et al.* 2006; Thorkelson *et al.* 2011).

### **Southernmost South America**

The Late Miocene to Pleistocene margin located south of the Chile triple junction (CTJ) in the southernmost South



America is similar in many characteristics to a transform continental margin.

The current tectonic framework of the southern Andean Cordillera involves a relatively complex interaction between the oceanic Nazca, Antarctic, and Scotia plates and the continental South American plate (Figure 4). The Nazca plate subducts rapidly beneath the South American plate at a relative velocity of 9 cm/yr, whereas the Antarctic plate subducts more slowly at 2 cm/yr. The Nazca and Antarctic plates are separated by the South Chile ridge (SCR) active spreading centre currently entering the subduction zone beneath the South American plate (Cande and Leslie 1986; Polonia *et al.* 2007; Breitsprecher and Thorkelson 2009; Lagabrielle *et al.* 2015, and references therein). In southern Chile, the extent of the slab is not well imaged due to a lack of significant subduction-related seismicity; as a result, the slab can only be traced to depths of  $\sim 40$  km adjacent to the CTJ using locally collected active source seismic profiles (Hayes *et al.* 2012, and references therein).

A gap in active volcanism occurs between 46–49°S in the region south of the CTJ (Stern *et al.* 1990).

The Austral Volcanic Zone (AVZ, 49–55°S) located more southward consists of five Holocene volcanoes of the South American plate (Stern and Kilian 1996; Stern 2004; Polonia *et al.* 2007) and the Cook volcano of the Scotia late near the Magallanes-Fagnano transform fault. There is no Benioff zone of seismic activity associated with the AVZ, and there is no information concerning pre-Holocene volcanic activity in this belt (Stern 2004). East of the AVZ, large Late Miocene to Pleistocene basaltic plateaus occur between 46.5°S and 52°S (e.g., Ramos and Kay 1992; Gorrington *et al.* 1997; D'Orazio *et al.* 2000, 2001; Gorrington and Kay 2001; Espinoza *et al.* 2005; Guivel *et al.* 2006; Boutonnet *et al.* 2010).

SCR-continental margin intersection is characterized by complex processes of collision and subduction. Since the ridge axis is trending 10° oblique to the orientation of the trench, the triple junction migrates northward (Forsythe and Nelson 1985; Cande and Leslie 1986; Forsythe *et al.* 1986; Cande *et al.* 1987; Bourgois *et al.* 2000; Lagabrielle *et al.* 2015).

Plate reconstructions based on subparallel oceanic magnetic anomalies along the coastline indicate that the initial SCR collision occurred near the southern tip of South America at (55°S) 15–14 Ma and has since migrated  $\sim 1000$  km northwards to its present location at the Taitao Peninsula at 46°S. Three distinct ridge-trench collision events have been identified. Between 14 and 10 Ma 700-km-long, a nearly continuous section of the SCR was collided between 55°S and 48°S. Shorter sections of the ridge, offset by large transform faults, were collided at 6 and 3 Ma between 48°S and 47°S (Cande and Leslie 1986). The initial stage of the SCR collision correlates with the cessation of the 16–14 Ma volcanic arc, emplacement of 14–12 Ma adakites behind it (Kay *et al.* 1993; Ramos *et al.* 2004; Espinoza *et al.* 2010), and formation of large volumes of Miocene (12 Ma) to Pleistocene mafic magmas erupted over vast areas of the southern Patagonian (e.g., Ramos and Kay 1992; Gorrington *et al.* 1997; D'Orazio *et al.* 2000, 2001; Gorrington and Kay 2001; Guivel *et al.* 2006). In Late Miocene (12 Ma), five granitoid plutons intruded along the N-trending lineament over 650 km long in the eastern edge of the main cordillera. This line of Miocene plutons strikes subparallel, with a divergence of approximately 15°, to the present trench and collided with the Miocene fragment of the SCR (Altenberger *et al.* 2003).

The modern orogenic belt of the Patagonian Cordillera formed from south to north during the continuous ridge collisions from 14 Ma (Ramos 2005, 2009; Goddard and Fosdick 2019) and in front of the 16–14 Ma volcanic arc, whose fragments are found in the present-

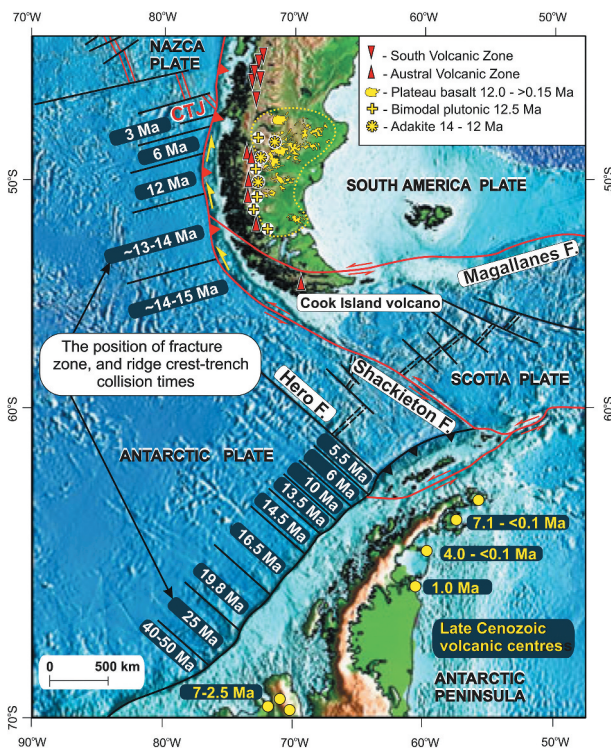


**Figure 4.** Late Cenozoic geodynamics and magmatic complexes of southernmost South America and the Antarctic Peninsula as a result of ridge-crest-trench intersection (collision) or change in the direction of oceanic plate movement or subduction. Compilation after Hole and Larter 1993; Gorrington and Kay 2001; Altenberger *et al.* 2003; Ramos *et al.* 2004; Eagles and Jokar 2014. The yellow arrows show migration of the Chile Triple Junction (CTJ) related to the transform margin. Red line with red triangles indicate the subduction zone, red line with red arrows indicate transform faults.



day back-arc region of Central Patagonia (Ramos *et al.* 2004; Espinoza *et al.* 2010, and references therein). Fault kinematic analysis and the N-S to N-NW trends of folds and thrusts both indicate dominant E-W compression with a component of right-lateral wrenching along the strike (Coutand *et al.* 1999). The Patagonian Cordillera shows morphotectonic and tectonic features, strongly differs from that of the northernmost Andes and is not expected in a normal subduction-related belt located away from a buried spreading centre (Ramos 2005, 2009; Scalabrino *et al.* 2010; Encinas *et al.* 2019; Georgieva *et al.* 2019, and references therein).

Despite the general understanding of Late Miocene–Pleistocene volcanic rock generation associated with the formation of the Patagonian slab window (slab-tear) (e.g., Ramos and Kay 1992; Gorrington *et al.* 1997, 2003; D’Orazio *et al.* 2000, 2001; Gorrington and Kay 2001; Espinoza *et al.* 2005; Guivel *et al.* 2006; Breitsprecher and Thorkelson 2009; Boutonnet *et al.* 2010), there are several models of their formation. The first model has been developed by Gorrington *et al.* (1997) to explain the sequence of magmatic events occurring along a SW–NE transect opposite the SCR segment that collided at ca. 12 Ma. This slab window has formed within the Nazca slab due to the volcanic rock position that was ~350 km away from the place where the SCR collided against the Chile trench. The close location (Cerro Pampa) of 14–12 Ma adakites and 12 Ma plateau basalts implies slab melting before slab window opening.

However, Guivel *et al.* (2006) argued that the subduction of the SCR at these latitudes (46–47°S) started at 6 Ma, whereas the emplacement of the main plateau basalts took place between 12.4 Ma and 5 Ma, which precludes a convincing cause–effect relationship. They proposed a model in which the collision of the southernmost segments of the SCR around 15 Ma caused a tear in the Nazca slab subparallel to the trench.

According to the model developed by Breitsprecher and Thorkelson (2009), the Patagonian slab window is a subsurface tectonic feature resulting from subduction of the Nazca–Antarctic spreading-ridge system beneath southern South America and the formation of a slab window below the overriding plate, created between the Nazca and Antarctic diverging plates. In this model, the majority of the slab window’s areal extent and geometry is controlled by the highly oblique (near-parallel) subduction angle of the Nazca–Antarctic ridge system and by the high contrast in relative convergence rates between these two plates relative to South America. This model of the slab-window does not explain why OIB basalts are located at 46–47°S. The authors appeal to a tear in the Nazca slab as the mechanism responsible for triggering mafic magmatism, as proposed by Guivel

*et al.* (2006), which continues to be a viable scenario (Breitsprecher and Thorkelson 2009).

Alternatively, Guillaume *et al.* (2013) proposed that complex mantle-flow patterns around the edges of the subducting slab may trigger lateral (i.e., trench-parallel) mantle flow, inducing remote alkaline volcanism and a large-scale thermal impact on the upper crust well before the arrival of the slab window. Georgieva *et al.* (2019) proposed an alternative model trench-orthogonal slab-tear for 46–47°S basalts. Such tears can initiate due to a lateral difference in thermal structure and strength within a subducting slab, possibly arising from the presence of a transform fault or fracture zone.

Movement of the CTJ from south to north along the continental margin, subparallel ridge-crest-trench collision, with simultaneous formation of Late Miocene–Pleistocene orogenic belt due to compression with a component of right-lateral wrenching, and absence of Late Miocene–Pleistocene subduction-related magmatic rocks allow it to be concluded that in this particular period in southern South America, the setting of the transform continental margin existed.

In southernmost South America, the following magmatic complexes related to the Late Miocene to Pleistocene continental transform margin have been revealed: adakites (14–12 Ma); Paine-type (K-rich) series of gabbros, monzodiorites and granitic plutons and dikes (12.5 Ma); and slab window or slab tear basalts (12 Ma to <0.1 Ma).

The porphyritic dacite of adakitic composition forms small (~100–200 m diameter) bodies in three areas along the eastern edge of the main cordillera (Kay *et al.* 1993; Ramos *et al.* 2004). Adakites show a systematic northward decrease of  $^{40}\text{Ar}/^{39}\text{Ar}$  in age  $14.50 \pm 0.29$ ,  $13.12 \pm 0.55$ , and  $11.39 \pm 0.61$  Ma, respectively (Ramos *et al.* 2004). In the north (Cerro Pampa), adakites erupted east of the inactive volcanic arc and in the area of consequent eruptions of OIB-type basalts. This association suggests that Nazca slab melting in Patagonia required a thermal input from the sub-slab asthenospheric mantle as well as a young hot subducting plate (Kay *et al.* 1993; Ramos *et al.* 2004).

Miocene intrusive complexes are located along a more than 650 km long N-trending lineament in southern Patagonia (Altenberger *et al.* 2003). These intrusives were built up by multiple pulses of gabbro-norites, hornblende-gabbros, monzodiorites and granitic rocks (Michael 1991; Michel *et al.* 2008; Leuthold *et al.* 2014, and references therein). Bulk rock geochemistry indicates that the different mafic units follow high-K calc-alkaline to shoshonitic differentiation trends characterized by variable alkali and H<sub>2</sub>O contents (Michael 1984, 1991; Altenberger *et al.* 2003; Leuthold *et al.* 2012, 2013).

High precision U-Pb zircon ID-TIMS dating on granite has shown that the granitic pulses were assembled between  $12.58 \pm 0.01$  and  $12.49 \pm 0.01$  Ma (Michel *et al.* 2008; Leuthold *et al.* 2012).

In the north of Late Cenozoic basal fields ( $46.5\text{--}49.5^\circ$  S), two periods of magmatism have been distinguished: (1) an older (12–5 Ma) voluminous, tholeiitic main-plateau sequence and (2) a younger (7 to  $<0.1$  Ma), less voluminous and more alkaline post-plateau sequence. Both main- and post-plateau lavas have strong OIB-like geochemical signatures (Ramos and Kay 1992; Gorrington *et al.* 1997; Gorrington and Kay 2001). Plio–Pleistocene (3–4–0.1 Ma) post-plateau basalts (at  $46.7^\circ$  S) have geochemical and isotopic signatures that are distinctive from most other lavas. These data are interpreted to indicate contamination of OIB-like asthenosphere-derived slab window magmas with the Paleoproterozoic lithospheric mantle (Gorrington *et al.* 2003). According to other authors, the Quaternary basalts ( $46\text{--}47^\circ$  S) display major elements, trace elements, and Sr and Nd isotopic features similar to those of oceanic basalts from the SCR and the CTJ near the Taitao Peninsula. Among 8.2–4.4 Ma-old main plateau basalts, there are the basalts that are still dominantly alkalic, displaying incompatible element signatures intermediate between those of OIB and arc magmas (Guivel *et al.* 2006). In the southernmost tip ( $\sim 52^\circ$  S) OIB-type subalkaline basalts and basaltic andesites erupted at 8.0–8.5 Ma from a series of five isolated buttes located at the southern end of the discontinuous belt of Late Cenozoic basaltic lava, and east of it, there is a large field of Pliocene (4 Ma)–recent OIB-type basalt (D’Orazio *et al.* 2000, 2001).

### West of the Antarctic Peninsula

West of the Antarctic Peninsula (see Figure 4), the transform continental margin has been related to the successive ridge-crest–trench collisions of segments of the Antarctic–Phoenix plate boundary from southwest to northeast that started in the Eocene time (Barker 1982; Hole 1990; Hole *et al.* 1991, 1994). A probable mechanism for the transform margin development at the north-western end of the Antarctic Peninsula requires either significant transtensional effects caused by the configuration and drift vector of the Scotia plate after the activity of the West Scotia ridge ceased at c. 7 Ma or rollback of the Phoenix plate under the South Shetland Islands after the cessation of spreading activity along the Phoenix ridge at 3.3–0.2 Ma, causing the north-western migration of the South Shetland trench (Solari *et al.* 2008).

Two distinct groups of latest Cenozoic (15 to  $<0.1$  Ma) OIB-like basalts are recognized along the Antarctic

Peninsula (Figure 4). Small volumes of undersaturated basanites, tephrites, alkali and olivine basalts and ‘within-plate’ tholeiites, which post-date the cessation of subduction as a result of ridge-crest–trench interactions by 40 to  $<10$  Ma, are scattered along much of the southern part of the peninsula. At James Ross Island, in the northern part of the peninsula, alkali basalts, hawaiites and rare mugearites erupted synchronously with subduction at the South Shetland Islands trench to the west. These two groups of basalts are remarkably similar in terms of their geochemical and isotopic characteristics, although they apparently owe their origin to two distinct combinations of tectonic processes. The southern Antarctic Peninsula basalts are causally related to the cessation of subduction, the formation of slab windows and the upwelling and decompressional melting of subslab asthenosphere. These suites of basalts were generated as a result of significant lithospheric extension and passive asthenospheric upwelling on a regional scale. In addition, there is no evidence for the existence of a mantle plume beneath the region (Hole 1990; Hole *et al.* 1991, 1994).

### Transform margin related to the changed direction of oceanic plate movement

#### Western Aleutian–Komandorsk

The transform margin of the western Aleutian–Komandorsk region between  $172^\circ$  E (west of Near Islands), and  $164^\circ$  E is essential for understanding of the Pacific-type transform margin origin. There, the transform margin formed not because of the spreading ridge subduction or collision but due to the changed direction of oceanic plate movement along the Aleutian Arc from subduction in the east to transform sliding in the west. As the active slab is not registered here; thus, there is no subduction (Hayes *et al.* 2012; Schellart and Rawlinson 2013; Petricca and Carminati 2016).

An important outcome of the WAVE and KALMAR cruises was the discovery of a 300-km-long zone of active seafloor volcanism west of Buldir Island, the location of the westernmost emergent volcano in the Aleutian arc (Yogodzinski *et al.* 2015). These and the data collected from Piip Seamount near Kamchatka Peninsula (Yogodzinski *et al.* 1995; Kelemen *et al.* 2003) helped to reveal an active volcanic front 700-km-long that spans from the Buldir Volcano to Piip Seamount in the Komandorsk area (Yogodzinski *et al.* 2015). The eastern part of these submarine volcanoes (Ingenstrom Depression) relates to the convergent margin, while its western part (Western Cones) relates to the transform margin.

The seafloor volcanism of the western Aleutian–Komandorsk transform margin is related to a very large window registered between 172°E, and 164°E and defined by the term slab portal (Levin *et al.* 2005). According to Kay *et al.* (2014), this slab portal is probably related to the lithosphere subducted before 6 Ma. Late Pleistocene rocks dredged from Piip Volcano represented by ‘Piip-type’ magnesian andesites (Yogodzinski *et al.* 1995). Lavas dredged from Western Cones volcanoes are primarily basalts, dacites and rhyodacites. Basalts have geochemical characteristics that differ from those typical of island arc basaltic lavas. High MgO and Mg# relative to silica, flat to decreasing abundances of incompatible elements, and decreasing Pb isotope ratios with increasing SiO<sub>2</sub> rule out an origin for the dacites and rhyodacites by fractional crystallization. The physical setting of some samples (erupted through the Bering Sea oceanic lithosphere) rules out an origin for their garnet rutile trace element signature by melting in the deep crust. Adakitic trace element patterns in the dacites and rhyodacites are therefore interpreted as the product of eclogite-facies melting of subducted oceanic lithosphere (Yogodzinski *et al.* 2015).

### **Southernmost tip of the Andes**

At the southernmost tip of the Andes, the boundary between the Antarctic and Scotia plates is located along the Chile trench and the Shackleton fracture zone, while the Scotia–South America plate boundary corresponds to the Magallanes–Fagnano fault system on land and to the North Scotia ridge to the east. The triple junction between these plates has been interpreted to be a diffuse area of deformation located west of the Strait of Magellan (Polonia *et al.* 2007, and references therein). The Antarctic plate convergence direction, which is nearly orthogonal at the latitude of the northernmost Lautaro volcano in the AVZ (49°S), becomes increasingly oblique along the Scotia plates and finally transits into the Shackleton fracture zone, which forms the left-lateral transform boundary (Sue and Ghiglione 2016; Santibáñez *et al.* 2019, and references therein).

Among the AVZ adakite volcanoes and arc volcanoes from a global perspective, Cook Island (54°S) Mg#-andesites (‘adakites’) are extraordinary in their MORB-like isotopic composition and certain MORB-like trace-element ratios which preclude crustal contamination. Ba/La (<5) is also significantly lower than typical arc magmas for which dehydration of subducted oceanic crust and contamination of the sub-arc mantle by alkali and alkaline-earth-element-rich hydrous fluids is considered an important petrogenetic process (Stern and Kilian 1996). Upon the result, Stern and Kilian (1996) proposed fragmentation of the subducted slab and deep

lithospheric faults. South of 52°S and in the area of the Cook volcano seismicity occurs mainly in the first 30 km of the crust, i.e., there is no deep seismicity typical of the subduction zones (Sue and Ghiglione 2016). This all probably means that the Cook volcano is related to a transform margin (Santibáñez *et al.* 2019).

### **Transform margin related to an island arc-continent collision**

#### **New Guinea island**

The present-day tectonics of the New Guinea region are the result of the Australian and Pacific plates’ oblique collision. At the end of the Late Miocene, the Australian continental plate moving north-north-eastern collided with Palaeogene-Miocene island arcs (Abbott *et al.* 1994; Hill and Hall 2003; Cloos *et al.* 2005; Baldwin *et al.* 2012). At the same time, when the Pacific plate was moving south–westward, the eastern part of the largest and thickest Ontong Java plateau (33 km) collided with the Solomon arc (e.g., Mann and Taira 2004; Taylor 2006). In map view, the AUS-PAC zone of deformation resembles a large left-lateral transform sigma clast, within which microplates evolved (Figure 5), which partially transformed into convergent boundaries in Pliocene–Pleistocene (Cloos *et al.* 2005; Baldwin *et al.* 2012, and references therein).

The transform margin of New Guinea Island is the result of Late Miocene (~7.5 Ma) oblique arc-continent collision and consequent movement of the Pacific/Caroline Plate west-north-western, parallel to the Australian plate boundary (e.g., Cloos *et al.* 2005). The seismic tomographic studies show no evidence of a subducted slab currently present beneath western New Guinea (e.g., Hall and Spakman 2015), but tomography beneath central and eastern New Guinea does show evidence for a south-dipping subducted slab (Tregoning and Gorbato 2004). This south-dipping slab is related to the present-day New Guinea trench, but is interpreted to have been active from at least ~9 Ma (based on a ~650 km slab and subduction rate of 7 cm/yr) or even earlier (Tregoning and Gorbato 2004) and may be associated with middle Miocene magmatism in New Guinea (Webb *et al.* 2020). Cloos *et al.* (2005) concluded that the trench has been reactivated as the latest tectonic adjustment associated with arc/fore-arc-continent collision. This conclusion corresponds to the deformation study of the Lengguru fold belt of Wandamen Peninsula in West Papua and U–Pb isotopic dating, which shows that the region underwent crustal extension and shortening within the last six million years, and after ca. 3 Ma, the Lengguru fold belt went into a phase of crustal extension. Aerial and satellite



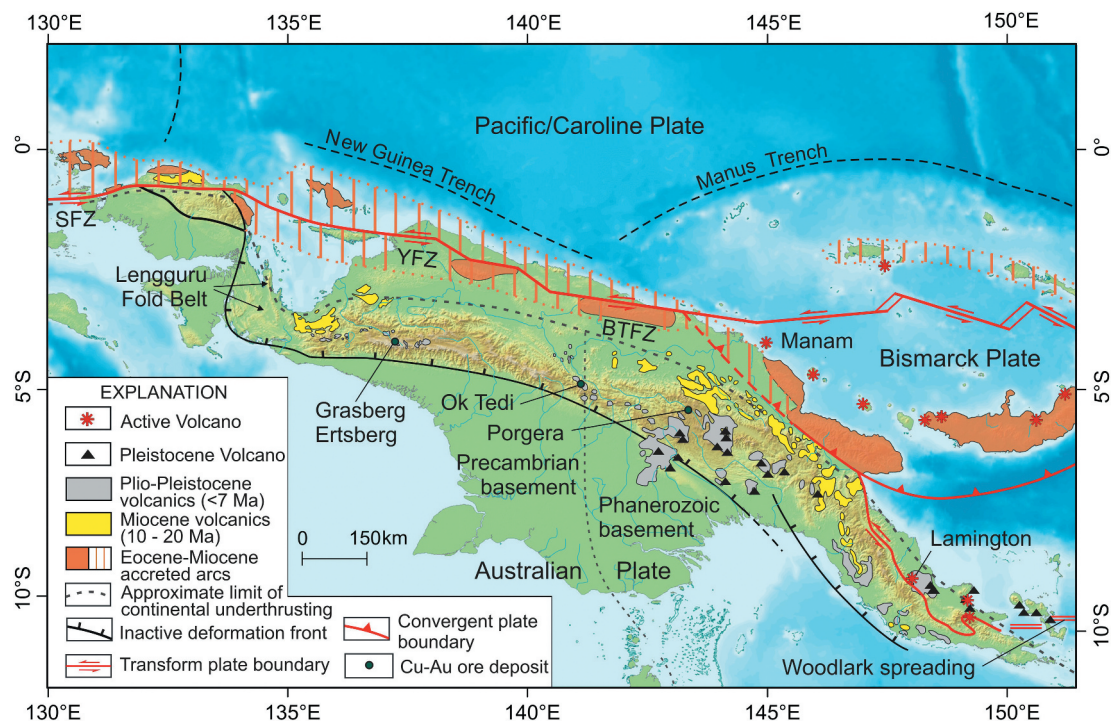


**Figure 5.** Late Cenozoic geodynamics and magmatic complexes of New Guinea Island resulting from island arc-continent collision (tectonic base and magmatic complexes after Cloos *et al.* 2005; Baldwin *et al.* 2012; Holm *et al.* 2019; Webb *et al.* 2020). BTFZ – Bewani-Torricelli fault zone; SFZ – Sorong fault zone; and YFZ – Yapen fault zone.

imagery also demonstrate that there is widespread evidence for relatively recent crustal extension throughout the Lengguru fold belt (White *et al.* 2019) that coincides with the initiation of major strike-slip faults (e.g., Pubellier and Ego 2002). Thus, we can assume that the Bewani-Torricelli fault zone (BTFZ), Sorong fault zone (SFZ) and Yapen fault zone (YFZ) represent transform plate boundary between the Pacific/Caroline Plate and New Guinea part of the Australian plate (see Figure 5), as shown in the global geophysical interpretations (e.g., Hayes *et al.* 2012; Petricca and Carminati 2016).

In south-eastern New Guinea, the fault zone separates the Woodlark microplate from the New Guinea highlands block of the Australian plate, linking via a series of left-lateral transfer faults from the Woodlark spreading centre rift to the Papuan peninsula. This fault zone is a reactivated megathrust that initially accommodated south-western obduction of the Papuan ophiolite during arc-continent collision. Active volcanoes of the Papuan peninsula are confined to this fault zone (Baldwin *et al.* 2012, and references therein).

Late Miocene (Pliocene, <7 Ma)–recent time syn- and postcollisional (Hamilton *et al.* 1983; McDowell *et al.* 1996; Cloos *et al.* 2005) or strike-slip related (e.g., Housh and McMahon 2000; Holm *et al.* 2015) volcanic and correlative intrusive rocks, generally intermediate in composition, occur scattered over >1000 km throughout

the New Guinea highlands block. In the highlands, some glaciated volcanoes were active in the Quaternary (Mackenzie and Johnson 1984). Plio–Pleistocene calc-alkaline basaltic-andesites also occur in the south-eastern part of New Guinea Island and D’Entrecasteaux Islands.

The youngest age of plutonic rocks was first dated Pliocene up to 2.5 Ma; however, SHRIMP U–Pb ages dated monzonite porphyry and monzodiorite of the Ok Tedi mining district to be approximately 1.4–1.1 Ma (van Dongen *et al.* 2010). Plio–Pleistocene magmatic rocks were erupted through deformed Australian continental margin sediments (Cloos *et al.* 2005). This magmatism is small in volume but of widely scattered occurrence. It is of considerable economic interest because giant porphyry copper/gold ore districts have so far been discovered in intrusive bodies (e.g., Cloos *et al.* 2005). Volcanic rocks are represented by potassic trachybasalt, tholeiitic basalt and trachyandesite (Mackenzie and Johnson 1984), intrusive gabbro, porphyry dominantly diorite, monzodiorite, monzonite and lamprophyre shoshonitic and high-K calc-alkaline suite (Housh and McMahon 2000; Cloos *et al.* 2005, and references therein). Mafic alkali intrusive complex has trace-element characteristics similar to those of basalts of intraplate settings (Richards 1990). It was proposed that Late Miocene–recent magmatism was

due to sub-slab asthenospheric upwelling into the tear rupturing of the subducting Australian lithosphere (McDowell *et al.* 1996; Cloos *et al.* 2005).

### Validation of discriminant diagrams

To make diagrams, we used the published data on the geochemical compositions of igneous rocks from recent geodynamic settings of model transform and convergent margins (see Figure 1 for the full details). Justifying the use of the database to determine further criteria of the geodynamic settings, we primarily based them on geological and geochronological characteristics of the magmatic complexes described in detail in the previous chapters. The geochemical database, for a total of more than 2400 analyses of various types of the rock compositions (see Supplementary data), includes the following:

Transform margin-related igneous rocks (1334 analyses):

*California and Baja California:* 1) the latest Oligocene to Middle Miocene basalt-rhyolite volcanic rocks, continental borderland of California (~39°N to ~33°N) (Sharma *et al.* 1991; Cole and Basu 1995; Weigand *et al.* 2002), 2) Pliocene to Quaternary basalt-rhyolite volcanic rocks, northern San Francisco Bay region (Schmitt *et al.* 2006; Sweetkind *et al.* 2011) and Late Miocene basalt to dacite lavas, Lava Mountains (Keenan 2000), 3) Late Miocene to Quaternary adakites, Nb-enriched basalts, tholeiitic and calc-alkaline basalts, basaltic andesites, andesites, dacites, rhyolites, alkali trachybasalts, and high-Mg# andesites, Baja California, Mexico (Luhr *et al.* 1995; Moreno and Demant 1999; Benoit *et al.* 2002; Pallares *et al.* 2007), 4) Late Miocene to Quaternary basalts and dacites, Basin and Range province (Coleman and Walker 1990; Ormerod *et al.* 1991; Farmer *et al.* 1995; Rogers *et al.* 1995; Henry and Aranda-Gomez 2000; Blondes *et al.* 2008).

*Queen Charlotte–Northern Cordilleran:* 1) Eocene tholeiitic and alkaline basalts, Olympic Peninsula, British Columbia (Babcock *et al.* 1992), 2) Eocene high-K calc-alkaline mafic and intermediate lavas of Buck Creek volcanic complex, central British Columbia (Dostal *et al.* 2001), 3) Eocene calc-alkaline basaltic andesite to rhyolite lavas with adakitic trace element signature including high-Mg# basaltic andesites, S British Columbia (Ickert *et al.* 2009), 4) Tertiary to recent alkaline basaltic lavas, the Northern Canadian Cordillera (Abraham *et al.* 2001, 2005); 5) Pleistocene alkaline to peralkaline mafic lavas (basanites and hawaiites) and more evolved trachytes and phonolites of Satah and Baldface Mountain volcanic fields, west-central British Columbia (Kuehn *et al.* 2015), 6) Pleistocene to Holocene basaltic rocks, the Isku-Unuk volcanic field; NW British Columbia (Cousens and Bevier

1995), 7) Quaternary alkaline basalts, Tasse areas, SE British Columbia (Friedman *et al.* 2016), 8) Tertiary sub-alkaline basaltic lavas of the Masset formation, the Queen Charlotte Islands (Hamilton and Dostal 2001).

*Southernmost South America:* 1) Late Miocene to Pleistocene tholeiitic to alkalic basalts and basaltic andesite plateau lavas, Patagonia, Argentina (Gorring and Kay 2001), 2) Late Miocene (14–12 Ma) andesitic to dacitic adakites, Cerro Pampa volcanic centre, the Patagonian Cordillera (Kay *et al.* 1993; Ramos *et al.* 2004), 3) Late Miocene (~12.5 Ma) Paine-type (K-rich) series of gabbros, monzodiorites and granitic plutons and dikes, Torres del Paine intrusive complex, southern Chile (Michael 1984, 1991; Leuthold *et al.* 2013; Müntener *et al.* 2018).

*West of the Antarctic Peninsula:* 1) Pliocene–Holocene tholeiite to alkali basalt and dolerite lavas and dikes, Seal Nunataks, the Antarctic Peninsula (Hole 1990; Hole and Larter 1993; Košler *et al.* 2009).

*Western Aleutian–Komandorsk:* 1) late Pleistocene and Holocene rhyodacites, and andesitic adakites from sea-floor volcanoes located west of Near Islands (172°E) to Piip Seamount (167.13°E) (Yogodzinski *et al.* 2015).

*Southernmost tip of the Andes:* 1) Holocene andesitic adakites, Cook Island (54°S) volcano (Stern and Kilian 1996).

*New Guinea Island:* 1) The latest Miocene–Pleistocene basalts to trachyandesites, and granite to granodiorite volcanic and igneous suites, Papua New Guinea highlands and NW New Guinea (Richards 1990; Richards and Ledlie 1993; Holm *et al.* 2015; Holm and Poke 2018; Webb *et al.* 2020).

Convergent (subduction) margin-related igneous rocks (1082 analyses): 1) the late Pleistocene–recent basalts and basaltic andesites from the Antuco volcano (37.4°S) to the Osorno volcano (41°S), the central southern volcanic zone of the Andes (Hickey-Vargas *et al.* 2016), 2) Quaternary volcanic rocks, the Aleutian arc, Alaska (Yogodzinski *et al.* 2015; Coombs *et al.* 2018), 3) late Pliocene basalts, basaltic andesites, dacites, rhyodacites, and rhyolites of the Karymskii and the Bol'shoi Semyachik volcanic massif, Kamchatka (Grib *et al.* 2009, Grib, E., 2015); Late Pleistocene andesitic to dacitic lava dome complex Bezymianny and Kliuchevskoi volcanoes (Almeev *et al.* 2013); recent basaltic andesites form the Avachinsky volcano, Kamchatka (Vicarò *et al.* 2012), 4) Quaternary volcanic rocks of the Kuril Island arc (Martynov *et al.* 2010) and Pleistocene basalts of Kunashir Island, Kuril Island arc (Martynov and Martynov 2017), 5) Quaternary lavas, NE Japan arc (Kimura and Yoshida 2006) and Oligocene to Quaternary basalts from the NE Japan arc (Shuto *et al.* 2015); Mio-Pliocene volcanic Izu–Bonin volcanic arc suite (Tamura 2002; The Database GEOROC with references therein); 6) Quaternary lavas, southern Pagan Island



lavas, Mariana arc (Marske *et al.* 2011), 7) Quaternary Java–Sunda front arc (Dempsey 2013), 8) recent volcanic rocks of the Tonga arc, SW Pacific (Hekinian *et al.* 2008) and the submarine Monowai volcanic centre, northern Kermadec arc, SW Pacific (Timm *et al.* 2011).

Slab window or slab tear environments are expected to differ from those involving normal subduction in patterns of subslab asthenospheric mantle flow, variations in mantle composition, flux of mantle-derived heat, and expressions of magmatism in both forearc and inboard regions (Dickinson and Snyder 1979a; Hole *et al.* 1991; Haeussler *et al.* 1995; Thorkelson 1996; Cloos *et al.* 2005; Pallares *et al.* 2007; Castillo 2008; Cole and Stewart 2009; Thorkelson *et al.* 2011). Primitive low-FeO\*/MgO, high-SiO<sub>2</sub> arc magmas are generally inferred as resulting from flux-melting of a peridotite mantle wedge and are characterized by high extents of mantle melting at high magmatic H<sub>2</sub>O contents. (e.g., Grove *et al.* 2003). Trace element patterns in subduction-related magmatic rocks show enrichments in large ion lithophile elements (K, U, Cs, Rb, Ba), and depletions in middle and heavy rare earth elements (MREE and HREE; Dy, Er, Yb, Lu) and in high field strength elements (HFSE; Ta, Nb, Zr, Hf) compared with mid-ocean ridge basalts (e.g., Gill 1981).

The slab tear or slab window may lead to the subslab asthenosphere rising through the tear (window) and adiabatically melting, and it invades the subcontinental lithospheric mantle and the overlying crust. Resulting melts derive through deep mantle processes likely include partial melting of the metabasaltic/gabbroic upper portion of the slab, leaving a garnet-bearing eclogitic residue. The magmas are derived from increasingly greater depths should be compositionally different than typical MORB, reflecting greater amounts of residual garnet (Hildebrand and Whalen 2017). Geochemistry of this slab window synextensional magmatism shows more MORB-like basalts towards the former fore-arc, and MORB-OIB-like basalts towards the former back-arc. Major elements show that slab window basalts reach TiO<sub>2</sub> values up to 3 wt%, as compared with the top value of 1.5 wt% of arc magmas. Besides, the MgO with respect to (FeO<sup>T</sup>+Al<sub>2</sub>O<sub>3</sub>) ratio helps to distinguish slab window magma changes from the former fore-arc to the former back-arc (Aragón *et al.* 2013).

It is assumed that they have alkaline and ferrous compositions with high contents of Ti, Nb, Ta, LREEs and LILEs. The strong partitioning of heavy rare earth elements (HREE) into residual garnet, rutile, allanite, etc., and the absence of Sr-plus Eu hosting plagioclase yields distinctive high La/Yb, Sm/Yb, Gd/Yb and Sr/Y ratios and the lack of negative Eu anomalies on chondrite normalized REE plots. The instability of a Ti-rich phase such as rutile plus residual garnet yields their high Nb/Y and Ta/Yb ratios

(Negrete-Aranda and Cañón-Tapia 2008; Thorkelson *et al.* 2011; Grebennikov *et al.* 2013; Grebennikov 2014; Hildebrand and Whalen 2017; Robinson *et al.* 2017).

When identifying the differences between the igneous rocks of supra-subduction island-arc and continental-margin type (related to convergent margins) and rocks formed in the setting of transform sliding of the lithospheric plates at the ocean margins we based on 'standard' geochemical criteria and existing diagrams. The geochemical data were filtered to eliminate evolved (high silica) compositions, which may reflect crustal rather than mantle sources, and samples with extreme trace element concentration, which may reflect analytical error, or misreporting of data. Therefore, the data have been interpreted with regards to the restrictions made by the authors: one should use only magmatic rocks with the total wt.% oxides near 98–101.5; ignore rocks subjected to considerable secondary superposed alterations with LOI ≥ 2 wt.%; and perform statistical processing of data in the 95% confidence interval for igneous rocks in order to achieve the maximum reliability of analytical results. To make the plots easy-to-work, no other filtering has been performed.

Data plotted in the existing standard diagrams (some of which are present in Figure 6) showed a significant overlapping of fields of convergent and transform margin igneous rocks, which is caused by the diversity of tholeiitic (subalkaline), alkaline or even calc-alkaline and peraluminous rocks typical of both geodynamic types.

Hence arose the necessity to find more informative discriminative diagrams to infer distinct geodynamic settings. Using the developed base of data collected at the most representative areas of these convergent and transform margins (see Supplementary data) we took into account the abundance or trends of each element reflected in term of magmatic processes that were discussed in multiple papers (Eby 1992; Abratis and Wörner 2001; Frost *et al.* 2001; Arculus 2003; Pearce *et al.* 2005; Aragón *et al.* 2013; Pearce 2014 etc.).

Having run multiple tests on the example of representative igneous rocks of convergent and transform margins we found informative ternary diagrams for petrogenic oxides TiO<sub>2</sub> × 10–Fe<sub>2</sub>O<sub>3</sub><sup>Tot</sup>–MgO, wt.%, and trace elements Nb\*5–Ba/La–Yb\*10, ppm (Figure 7A) and defined the field limits based on visually manipulating the boundaries to maximize correspondence to the available data (Figure 7B).

We use Ti, Mg, and Fe (II and III) oxides as a proxy to distinguish slab window magma changes (e.g., Aragón *et al.* 2013). As an indicator of the anhydrous character of the magmas, Nb is subduction-immobile in most arc systems, with the result that the vast majority of supra-subduction zone lavas have high Th/Nb (Pearce 2014). As

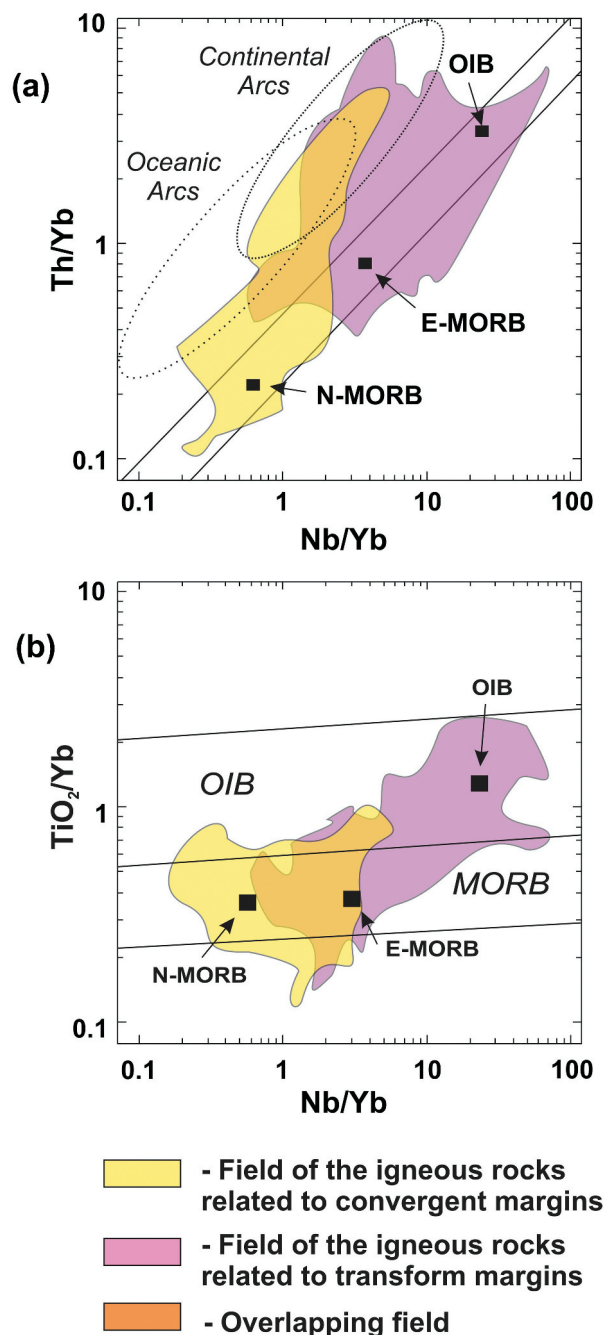


**Figure 6.** (A) Nb/Yb – Th/Yb, and Nb/Yb –  $\text{TiO}_2/\text{Yb}$  (B) discriminant diagrams to fingerprint tectonic settings (Pearce 2008, 2014). Field of the igneous rocks related to convergent and transform margins based on Supplementary data (see references therein).

a result, within-plate granites enriched in Nb have geochemical features that reflect enriched mantle sources and anhydrous crystallization (Pearce 1996). Yb is particularly suitable as it is strongly compatible with eclogitic assemblages and so is one of the most subduction-immobile incompatible elements. It can vary significantly during partial melting, but not in most oceanic subduction systems where the shallow depth and high degree of

melting rarely result in residual garnet (Pearce *et al.* 2005; Pearce 2014). Ba/La ratios in arc magma sources, by contrast, are highly susceptible to contributions from a dehydrating subducted slab (Abratis and Wörner 2001).

As seen in the presented diagrams, the points depicting rock compositions ( $\text{SiO}_2 < 63$  wt.%) form two main fields that almost do not overlap. The first field corresponds to igneous rocks from zones of the supra-subduction island arc and marginal continental magmatic types (related to convergent margins); the second field corresponds to magmatic rocks from the tectonic setting of transform continental or island arc margins (related to transform margins). When discriminating these rocks, it is recommended using both types of diagrams for the identification of their geodynamic positions to avoid ambiguous results that distort the geochemical compositions due to superimposed processes of assimilation, or contamination as well as low precision method results.

Some difficulties are posed by the separation of high-silica igneous rocks present both at convergent and transform margins. More siliceous rocks ( $\text{SiO}_2 > 63$  wt.%) are characterized by a certain overlapping (up to 10%, 42 from 445 samples) of the denoted fields on the  $\text{TiO}_2 \times 10 - \text{Fe}_2\text{O}_3^{\text{Tot}} - \text{MgO}$  diagram (Figure 7C), which is largely because the processes of siliceous magma generation are identical for both types and are followed by crustal assimilation in these geodynamic settings (e.g., Savov *et al.* 2009; Seitz *et al.* 2018). The geochemistry of rhyolites correlates strongly with the nature of the underlying basement terranes (Savov *et al.* 2009). Thus, the high silica end of the spectrum is much more complicated and needs even further filtering as well as careful consideration in the future. Notably, trace element concentrations show minimum overlapping on the  $\text{Nb} \times 5 - \text{Ba}/\text{La} - \text{Yb} \times 10$  plot. Summarizing the aforesaid, we may propose the use of additional geochemical criteria for these acidic-type rocks. It is necessary to recognize that convergent margin-related igneous rocks with siliceous compositions do not plot in the fields of geochemical A-type granites and related volcanic rocks but correspond to I-type granites (Whalen *et al.* 1987; Grebennikov 2014). Moreover, when constructing the geodynamic diagrams, more precise conclusions can be drawn with the use of geochemical compositions that include all silica types of coeval differentiates of magmatic melts.

### Testing of new discrimination plots

Examination of the new discrimination plots for the most debatable origin regions in relation to our article's objective (Figure 8 and Supplementary data) demonstrates excellent discrimination between magmatic rocks of

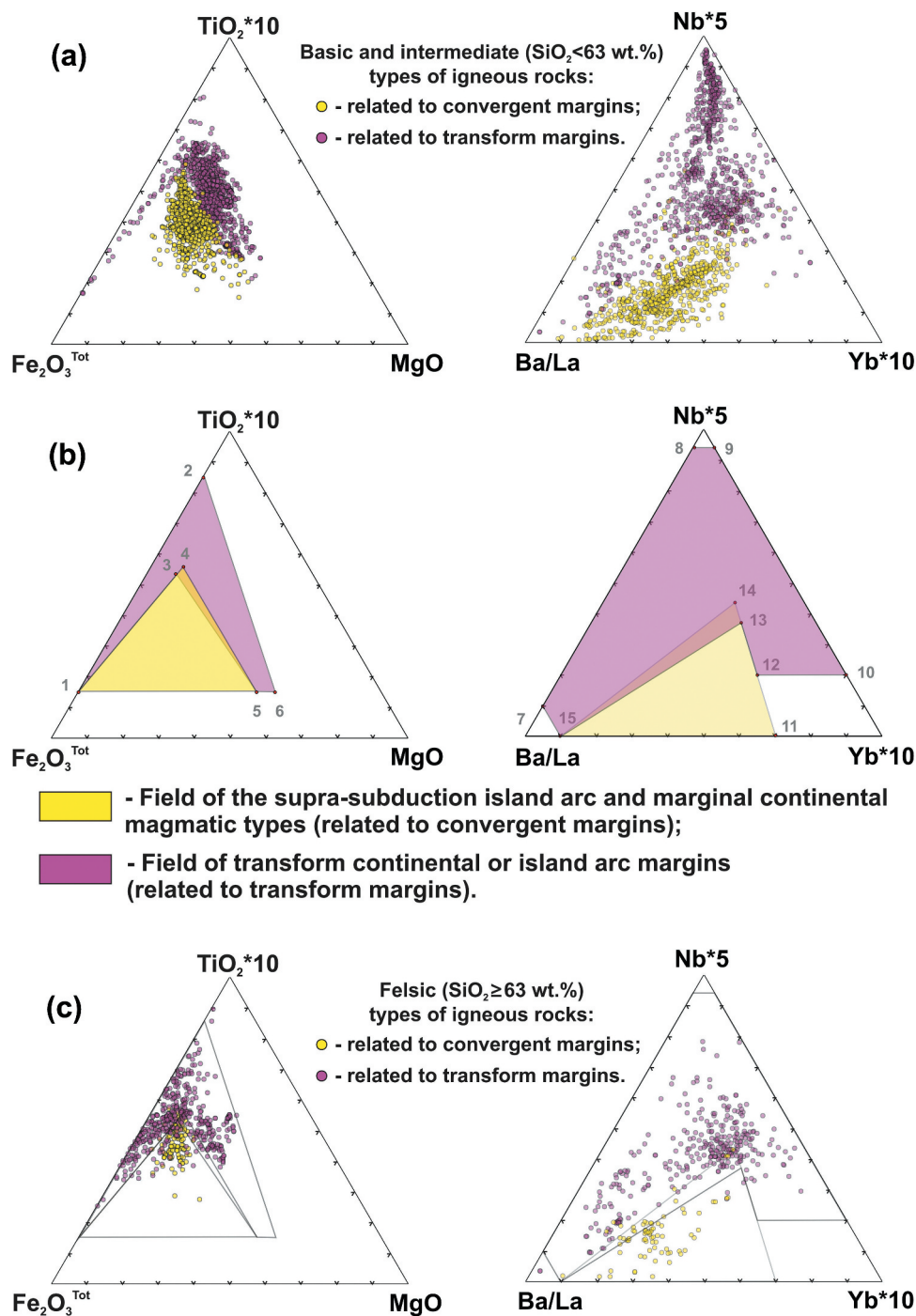


**Figure 7.**  $\text{TiO}_2 \times 10$ – $\text{Fe}_2\text{O}_3^{\text{Tot}}$ – $\text{MgO}$  and  $\text{Nb}^*5$ – $\text{Ba/La}$ – $\text{Yb}^*10$  discriminant diagrams for interpretation of geodynamic settings of the supra-subduction island arc and continental marginal types of magmatism (related to convergent margins) and transform sliding of lithospheric plates at ocean margins (related to transform margins). See the text, Supplementary data and references therein for the full details. Coordinates for plot fields (B) are based on these values: 1 (15; 85; 0), 2 (85; 15; 0), 3 (53; 38; 8), 4 (56; 35; 9), 5 (15; 35; 50), 6 (15; 30; 55), 7 (10; 90; 0), 8 (95; 5; 0), 9 (95; 0; 5), 10 (20; 0; 80), 11 (0; 30; 70), 12 (20; 25; 55), 13 (37; 21; 42), 14 (44; 19; 37), and 15 (0; 90; 10).

the supra-subduction island arc and continental marginal types of magmatism (related to convergent margins) and transform sliding of lithospheric plates at ocean margins (related to transform margins).

#### **Western Aleutian-Komandorsk (304 analyses):**

Volcanic rocks from the Western Cones (172°E) and Piip Seamount (167°E) distinguish from Aleutian volcanic rocks. Former ones on the proposed plots correspond to volcanic

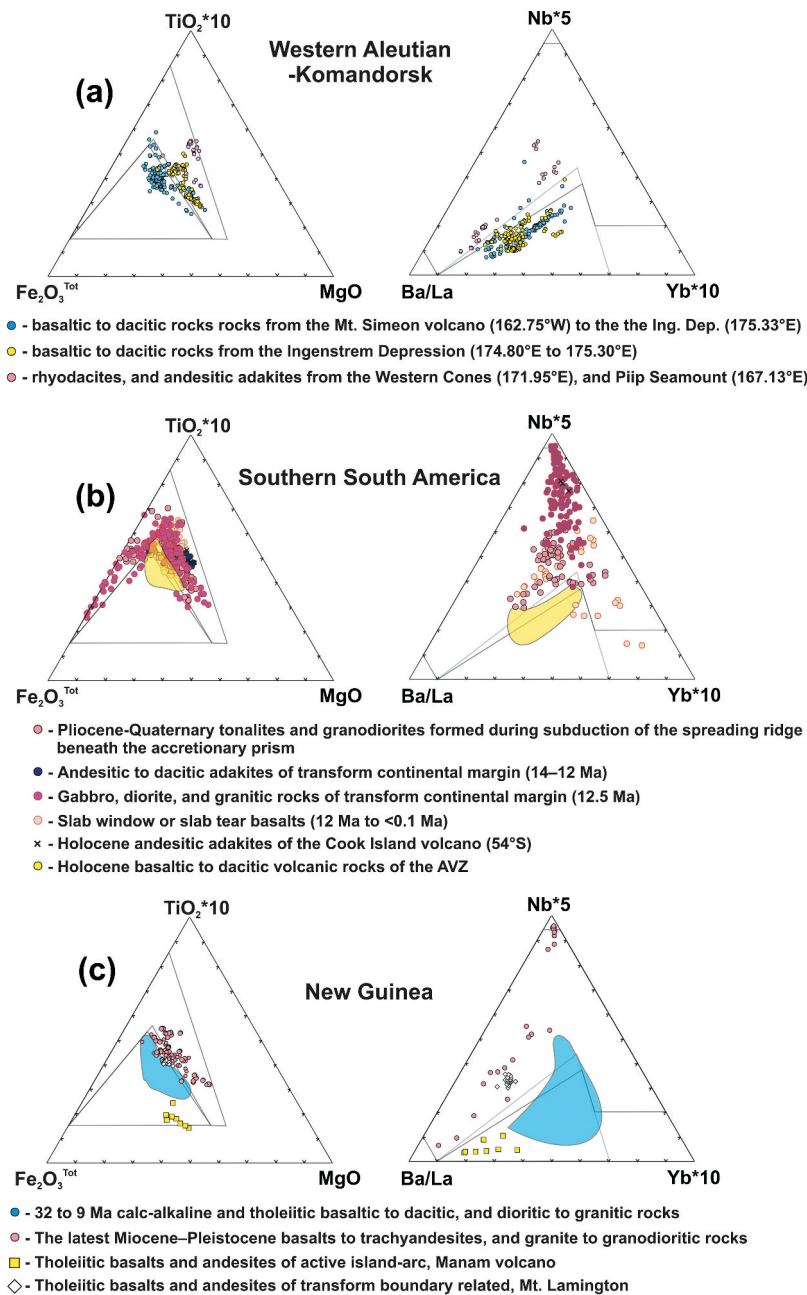


**Figure 8.**  $\text{TiO}_2 \times 10$ – $\text{Fe}_2\text{O}_3^{\text{Tot}}$ – $\text{MgO}$  and  $\text{Nb}^*5$ – $\text{Ba/La}$ – $\text{Yb}^*10$  discriminant diagrams for igneous rocks of the Aleutian arc (A), the southern South America (B) and New Guinea (C). The whole-rock major and trace elements are from Michael 1984, Michael, P.J., 1991; Johnson *et al.* 1985; Kaeding *et al.* 1990; Richards 1990; Kay *et al.* 1993; Richards and Ledlie 1993; Stern and Kilian 1996; Guivel *et al.* 1999, 2003; Gorrington and Kay 2001; D’Orazio *et al.* 2003; Ramos *et al.* 2004; Guivel *et al.* 2006; Kon *et al.* 2013; Leuthold *et al.* 2013; Holm *et al.* 2015; Yogodzinski *et al.* 2015; Zhang *et al.* 2015; Holm and Poke 2018; Müntener *et al.* 2018; Webb *et al.* 2020. See the text and Supplementary data for the full details. Coordinates for plot fields as for Figure 7.

rocks derived in the tectonic setting of transform island arc margins (related to transform margins), as the latter corresponds to the field of supra-subduction island arc and marginal continental magmatic rock types (Figure 8A). These results, which are consistent with the modelling of the Aleutian slab shape and the existence of a very large

window, ‘slab portal’ in the western part (Levin *et al.* 2005), clearly indicate that Ingenstrem Depression (174.80°E to 175.33°E) is a key area between the western Aleutian strike-slip zone and eastern subduction zone. As a result, the igneous rocks of Ingenstrem Depression show intermediate positions on the empirical fields (Figure 8A).



### **Southern South America (452 analyses):**

The Late Miocene to Pleistocene igneous rocks of southern South America differ from the Holocene volcanic rocks of the AVZ (with the exception of rocks from the Cook Island volcano) and correspond to magmatic rocks formed in the transform continental margin environment (Figure 8B and Supplementary data). Pliocene–Quaternary magmatic rocks have formed due to the heating of the accretionary prism by the Chile spreading ridge ('blowtorch' effect) and are also plotted within the transform margin field (Kaeding *et al.* 1990; Lagabrielle *et al.* 1994, 2000; Kon *et al.* 2013).

### **New Guinea (124 analyses):**

On discriminant diagrams (Figure 8C), the latest Miocene–Pleistocene volcanic and igneous suites of New Guinea related to the transform margin are separated from Oligocene–Miocene convergent margin suites and the active island-arc Manam volcano (Supplementary data). The rocks of the Mt. Lamington volcano are similar to the rocks of the transform margin. This signature agrees with the fact that Mt. Lamington lavas do not show the expected  $^{10}\text{Be}$  excess of recently subducted sediments (Gill *et al.* 1993).

### **Adakites (181 analyses):**

Adakites were first documented in the Aleutian arc (Kay 1978) and then were initially defined by Defant and Drummond (1990), as a distinct arc rock type (lava with 54 to 65 wt%  $\text{SiO}_2$  and  $\text{Mg\#} > 0.45$  and high  $\text{Sr/Y}$  and  $\text{La/Yb}$  ratios) produced specifically through melting of young subducted oceanic basalt. These rocks were also found among the post-arc (post-subduction) rock at Baja California transform continental margin where they are considered to be the result of the partial melting of the edges of the slab tear, which formed inside of the subducted Farallon plate after the cessation of subduction (e.g., Aguillón-Robles *et al.* 2001; Calmus *et al.* 2008; Castillo 2008). Adakite-like rocks produced through other petrogenetic processes also exist, and these may be more widespread than adakites (e.g., Martin *et al.* 2005; Castillo Castillo, P.R., 2012). Experimental evidence has demonstrated that high-pressure melting of a metabasaltic composition under the control of residual minerals, such as amphibole, garnet, clinopyroxene, and rutile, can account for the geochemical signature of most of the adakite suites irrespective of the tectonic setting of formation (Rossetti *et al.* 2014 and references therein).

In the discriminant diagrams, the compositions of high  $\text{Mg\#}$  volcanic rocks with adakitic affinity (Figure 9A) form two different empirical fields that almost do not overlap for petrogenic oxides (Figure 9B). The Cook Island adakites differ from the convergent margin adakitic rocks of the AVZ but are similar to the transform margin-related adakites of Patagonian and Western Aleutian ones (Supplementary data). Thus, we can assume that these diagrams can identify adakites related to a slab melting around the edges of the slab tear or slab window margins caused by subslab asthenospheric mantle input (Kay *et al.* 1993; Stern and Kilian 1996; Ramos *et al.* 2004; Thorkelson and Breitsprecher 2005; Calmus *et al.* 2008; Castillo 2008) and adakites of a slab melting at the stage of subduction (e.g., Smith and Leeman 1987; Stern and Kilian 1996; Nakamura and Iwamori 2013). At the same time, in trace elements ternary diagram compositions of adakites related to a slab melting at the stage of subduction fall into field of transform margin magmatism (Figure 9C). As it can be seen from Supplementary data, their high  $\text{Ba/La}$  ratios ( $\sim 10$ –90) and low  $\text{Nb/Zr}$  ratios (0.03–0.09) suggest derivation from a fluid-modified, depleted-mantle wedge, as is typical of 'normal' arc magmatism (see Abratis and Wörner 2001). This also evidenced by low  $\text{Ti/Yb}$  ratios that resulted from the melting of depleted mantle under shallow, hydrous conditions (see Pearce 2008, 2014 and references therein). On the other hand, Keskin (2007) pointed out that lavas containing a distinct subduction signature have consistently higher  $\text{Th/Ta}$  ratios and, in general, lower Ta concentrations compared to post-collisional slab break-off related lavas. This type of adakites, however, have even lower  $\text{Th/Ta}$ , and similar  $\text{Nb/Yb}$  ratios comparable to adakites related to slab tearing. Such ambiguous geochemical characteristics along with diagrams results (Figure 9D) emphasize once again that adakites are a very problematic/peculiar rock-type and their genesis is still unknown.

It should be noted, though, we do not discuss the genesis problem of these high- $\text{Mg\#}$  volcanic rocks with adakitic affinity but test the new discrimination plots with only true adakites (following Defant and Drummond 1990; Martin 1999) derived from subduction and post-subduction scenarios resulting from the slab melting. Obtained results confirm once more that both types of proposed diagrams should be used for identification of geodynamic positions.

In summary of 'Testing of new discrimination plots' section, it should be recalled that analysis of the data on the presented ternary diagrams permits us to relate, with some caution, igneous complexes to a particular geodynamic setting. However, no diagram is as informative for understanding the genesis



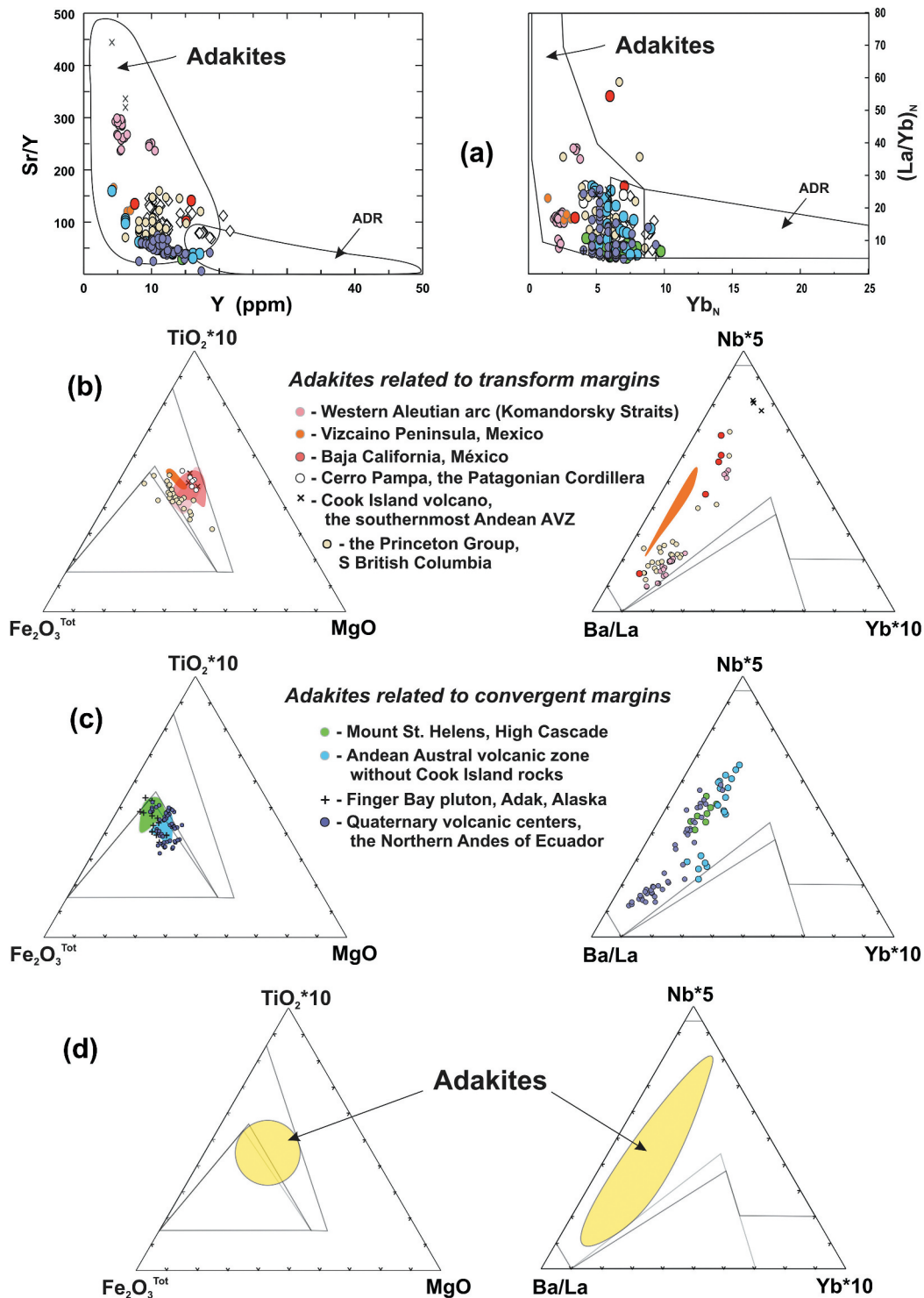


**Figure 9.** Sr/Y vs. Y and (La/Yb)<sub>N</sub> vs. Yb<sub>N</sub> plots (following Defant and Drummond 1990, and Martin 1999) that are typically used to distinguish adakites from normal arc andesite, dacite and rhyolite (ADR) lavas (A); TiO<sub>2</sub> × 10–Fe<sub>2</sub>O<sub>3</sub><sup>Tot</sup>–MgO and Nb\*5–Ba/La–Yb\*10 discriminant diagrams for true adakites derived from post-subduction (B), and subduction scenarios (C). Generalized discriminant diagrams for true adakites related to convergent and transform margins (D). The whole-rock major and trace elements are from Kay *et al.* 1983; Smith and Leeman 1987; Kay *et al.* 1993; Stern and Kilian 1996; Aguilón-Robles *et al.* 2001; Benoit *et al.* 2002; Ramos *et al.* 2005; Pallares *et al.* 2007; Chiaradia *et al.* 2009; Ickert *et al.* 2009; Yogodzinski *et al.* 2015. See the text and Supplementary data for the full details. Coordinates for plot fields as for Figure 7.

and geodynamic setting of formation of igneous rocks as a comprehensive analysis of data on their

composition, isotope properties, structural position, and age. Therefore, these diagrams are proposed as

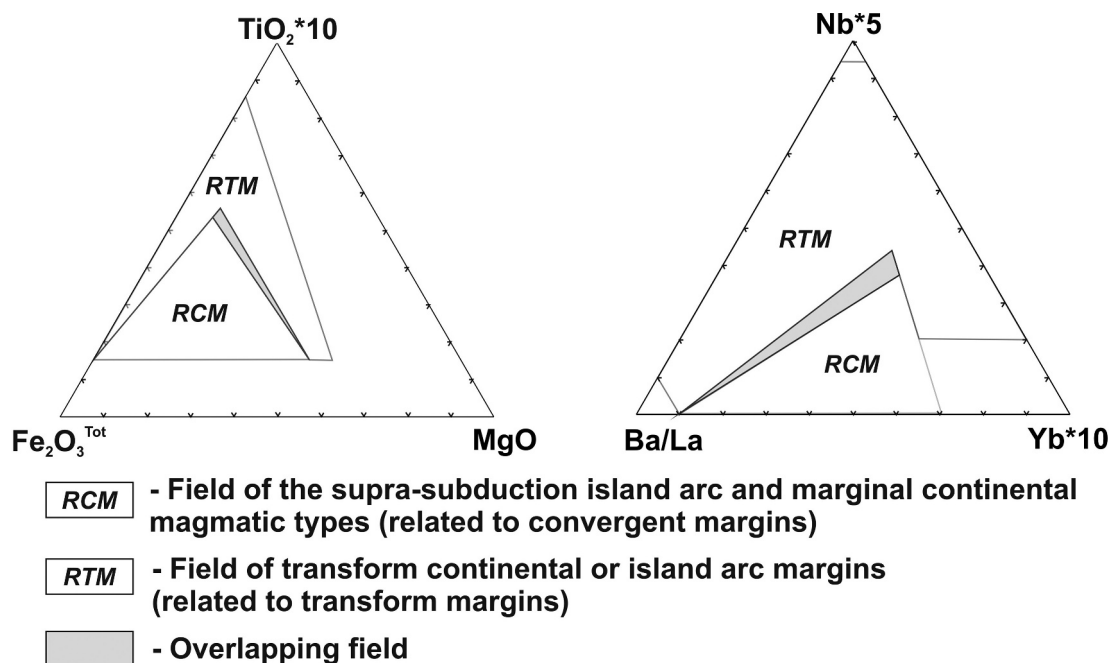


**Figure 10.**  $\text{TiO}_2 \times 10$ – $\text{Fe}_2\text{O}_3^{\text{Tot}}$ – $\text{MgO}$  and  $\text{Nb} \times 5$ – $\text{Ba/La}$ – $\text{Yb} \times 10$  discriminant diagrams for interpretation of geodynamic settings of the supra-subduction island arc and continental marginal types of magmatism (related to convergent margins) and transform sliding of lithospheric plates at ocean margins (related to transform margins). Coordinates for plot fields as for Figure 7.

one of the tools for a comprehensive analysis of geological data.

### Concluding remarks

Based on the analysis conducted with up-to-date geological and geophysical data, the following points can be concluded. Cenozoic geodynamics of the Pacific Rim relate to a convergent or transform margin. Transform margins represent lithospheric plate boundaries with horizontal sliding of the oceanic plate, which in time and space replaced the subduction-related convergent margins. Transit from a convergent to transform margin along a continent or island arc is conditioned by the changes in oceanic plate interaction. For transform margins of different types, intensive strike-slip tectonics and post-subduction magmatism related to the slab window or slab tear formation are common. The slab window is a result of spreading ridge collision (subduction) with a continental margin and consequent divergence of slabs beneath a continent. Ridge-crest-trench intersection can take place together with triple junction migration along continental margins. Slab tear formed as a result of active subslab asthenosphere upwelling through the stalled (fossil) slab after subduction cessation due to the following different factors: 1) ridge death along continental margin; 2) change in the direction of oceanic plate movement; and 3) island arc-continent collision. Slab tear can also form beneath the continent

away from the paleotrench simultaneously with slab window ridge-crest-trench intersection.

Igneous rocks formed above the slab window or slab tear are similar in composition. Geochemical diversity of transform margin igneous rocks is determined by their location in the former forearc to the former back-arc regions.

The comprehensive geochemical dataset for volcanic and plutonic rocks from the model transform and convergent geodynamic settings allowed us to build the ternary diagrams for petrogenic oxides  $\text{TiO}_2 \times 10$ – $\text{Fe}_2\text{O}_3^{\text{Tot}}$ – $\text{MgO}$  (wt.%) and trace elements  $\text{Nb} \times 5$ – $\text{Ba/La}$ – $\text{Yb} \times 10$  (ppm). New discrimination plots (Figure 10) add more information to the previous studies and show distinctive features for igneous rocks of calc-alkaline mafic, intermediate, felsic and adakitic composition present on both convergent and Pacific-type transform margins.

### Acknowledgments

We are grateful to Evgeniy V. Sklyarov (Institute of the Earth's Crust, Irkutsk), Ivan Savov (University of Leeds), David W. Scholl (USGS Pacific Coastal & Marine Science Centre), and one anonymous reviewer for helpful comments on earlier versions of the manuscript. Finally, we would like to thank Federico Lucci (Department of Science, Rome, Italy), Robert J. Stern (Editor-in-Chief, International Geology Review), and one more

anonymous reviewer for providing detailed and insightful reviews that have greatly improved this manuscript.

## Disclosure statement

The authors declare that they have no conflict of interest.

## References

- Abbott, L.D., Silver, E.A., and Galewsky, J., 1994, Structural evolution of a modern arc-continent collision in Papua New Guinea, *Tectonics*, v. 13, no. (5), p. 1007–1034. [10.1029/94TC01623](#)
- Abraham, A.-C., Francis, D., and Polvé, M., 2001, Recent alkaline basalts as probes of the lithospheric mantle roots of the Northern Canadian Cordillera, *Chemical Geology*, v. 175, no. (3–4), p. 361–386. [10.1016/S0009-2541\(00\)00330-2](#)
- Abratis, M., and Wörner, G., 2001, Ridge collision, Slab-window Formation, and the Flux of Pacific Asthenosphere into the Caribbean Realm, *Geology*, v. 29, no. (2), p. 127–130. [10.1130/0091-7613\(2001\)029<0127:RCSWFA>2.0.CO;2](#)
- Abraham, A.-C., Francis, D., and Polvé, M., 2005, Origin of Recent Alkaline Lavas by Lithospheric Thinning beneath the Northern Canadian Cordillera, *Canadian Journal of Earth Sciences*, v. 42, no. (6), p. 1073–1095. [10.1139/e04-092](#)
- Aguillón-Robles, A., Calmus, T., Benoit, M., Bellon, H., Maury, R. C., Cotten, J., Bourgois, J., and Michaud, F., 2001, Late Miocene adakites and Nb-enriched basalts from Vizcaino Peninsula, Mexico: Indicators of East Pacific Rise Subduction below Southern Baja California?, *Geology*, v. 29, no. (6), p. 531–534. [10.1130/0091-7613\(2001\)029<0531:LMAANE>2.0.CO;2](#)
- Almeev, R.R., Kimura, J.-I., Ariskin, A.A., and Ozerov, A.Y., 2013, Decoding crystal fractionation in calc-alkaline magmas from the Bezymianny Volcano (Kamchatka, Russia) Using Mineral and Bulk Rock Compositions, *Journal of Volcanology and Geothermal Research*, v. 263, p. 141–171. [10.1016/j.jvolgeores.2013.01.003](#)
- Altenberger, U., Oberhänsli, R., Putlitz, B., and Wemmer, K., 2003, Tectonic controls and Cenozoic magmatism at the Torres del Paine, Southern Andes (Chile, 51°10'S), *Revista Geológica de Chile*, v. 30, no. (1), p. 6581. [10.4067/S0716-02082003000100005](#)
- Aragón, E., Pinotti, L., Fernando, D., Castro, A., Rabbia, O., Coniglio, J., Demartis, M., Hernando, I., Cavarozzi, C.E., and Aguilera, Y.E., 2013, The Farallon-Aluk ridge collision with South America: Implications for the geochemical changes of slab window magmas from fore-to back-arc, *Geoscience Frontiers*, v. 4, (4), p. 377–388. [10.1016/j.gsf.2012.12.004](#)
- Arculus, R.J., 2003, Use and Abuse of the Terms Calcalkaline and Calcalkalic, *Journal of Petrology*, v. 44, no. (5), p. 929–935. [10.1093/ptrology/44.5.929](#)
- Atwater, T., 1970, Implications of plate tectonics for the Cenozoic tectonic evolution of Western North America, *Geological Society of America Bulletin*, v. 81, no. (12), p. 3513–3536. [10.1130/0016-7606\(1970\)81\[3513:IOPTFT\]2.0.CO;2](#)
- Babcock, R.S., Burmester, R.F., Engebretson, D.C., Warnock, A., and Clark, K.P., 1992, A rifted margin origin for the crescent basalts and related rocks in the Northern Coast Range Volcanic Province, Washington and British Columbia, *Journal of Geophysical Research*, v. 97, no. (B5), p. 6799–6821. [10.1029/91JB02926](#)
- Baldwin, S.L., Fitzgerald, P.G., and Webb, L.E., 2012, Tectonics of the New Guinea region, *Annual Review of Earth and Planetary Sciences*, v. 40, no. (1), p. 495–520. [10.1146/annurev-earth-040809-152540](#)
- Barker, P.F., 1982, The Cenozoic subduction history of the Pacific margin of the Antarctic Peninsula: Ridge crest–trench interactions, *Journal of the Geological Society*, v. 139, no. (6), p. 787–801. [10.1144/gsjgs.139.6.0787](#)
- Basile, C., 2015, Transform continental margins—part 1: Concepts and models, *Tectonophysics*, v. 661, p. 1–10. [10.1016/j.tecto.2015.08.034](#)
- Batiza, R., 1977, Petrology and chemistry of Guadalupe Island: An alkalic seamount on a fossil ridge crest, *Geology*, v. 5, no. (12), p. 760–764. [10.1130/0091-7613\(1977\)5<760:PACOGI>2.0.CO;2](#)
- Benoit, M., Aguillon-Robles, A., Calmus, T., Maury, R.C., Bellon, H., Cotten, J., Bourgois, J., and Michaud, F., 2002, Geochemical diversity of Late Miocene volcanism in southern Baja California, Mexico: Implication of Mantle and Crustal Sources during the Opening of an Asthenospheric Window, *The Journal of Geology*, v. 110, no. (6), p. 627–648. [10.1086/342735](#)
- Blondes, M.S., Reiners, P.W., Ducea, M.N., Singer, B.S., and Chesley, J., 2008, Temporal–compositional trends over short and long time-scales in basalts of the big pine volcanic field, California, *Earth and Planetary Science Letters*, v. 269, no. (1–2), p. 140–154. [10.1016/j.epsl.2008.02.012](#)
- Bohannon, R.G., and Parsons, T., 1995, Tectonic implications of post–30 Ma Pacific and North American relative plate motions, *Geological Society of America Bulletin*, v. 107, no. (8), p. 937–959. [10.1130/0016-7606\(1995\)107<0937:TIOPMP>2.3.CO;2](#)
- Bourgois, J., Guivel, C., Lagabriele, Y., Calmus, T., Boulègue, J., and Daux, V., 2000, Glacial-interglacial trench supply variation, spreading-ridge subduction, and feedback controls on the Andean margin development at the Chile triple junction area (45–48°S), *Journal of Geophysical Research: Solid Earth*, v. 105, no. (B4), p. 8355–8386. [10.1029/1999JB900400](#)
- Boutonnet, E., Arnaud, N., Guivel, C., Lagabriele, Y., Scalabrino, B., and Espinoza, F., 2010, Subduction of the South Chile active spreading ridge: A 17Ma to 3Ma magmatic record in central Patagonia (Western edge of Meseta del Lago Buenos Aires, Argentina), *Journal of Volcanology and Geothermal Research*, v. 189, no. (3–4), p. 319–339. [10.1016/j.jvolgeores.2009.11.022](#)
- Breitsprecher, K., and Thorkelson, D.J., 2009, Neogene kinematic history of Nazca–Antarctic–Phoenix slab windows beneath Patagonia and the Antarctic Peninsula, *Tectonophysics*, v. 464, no. (1–4), p. 10–20. [10.1016/j.tecto.2008.02.013](#)
- Breitsprecher, K., Thorkelson, D.J., Groome, W.G., and Dostal, J., 2003, Geochemical confirmation of the Kula–Farallon slab window beneath the Pacific Northwest in Eocene time, *Geology*, v. 31, no. (4), p. 351–354. [10.1130/0091-7613\(2003\)031<0351:GCOTKF>2.0.CO;2](#)
- Bryan, S.E., Orozco-Esquivel, T., Ferrari, L., and López-Martínez, M., 2014, Pulling Apart the Mid to Late Cenozoic Magmatic Record of the Gulf of California: Is There a Comodonu Arc? *Geological Society, London, Special Publications*, v. 385, no. (1), p. 389–407. [10.1144/SP385.8](#)

- Calmus, T., Aguillón-Robles, A., Maury, R.C., Bellon, H., Benoit, M., Cotten, J., Bourgois, J., and Michaud, F., 2003, Spatial and temporal evolution of basalts and magnesian andesites ("bajaites") from Baja California, Mexico: The role of slab melts, *Lithos*, v. 66, no. (1–2), p. 77–105. [10.1016/S0024-4937\(02\)00214-1](#)
- Calmus, T., Pallares, C., Maury, R.C., Aguillón-Robles, A., Bellon, H., Benoit, M., and Michaud, F., 2011, Volcanic markers of the post-subduction evolution of Baja California and Sonora, Mexico: Slab Tearing versus Lithospheric Rupture of the Gulf of California, *Pure and Applied Geophysics*, v. 168, p. 1303–1330. [10.1007/s00024-010-0204-z](#)
- Calmus, T., Pallares, C., Maury, R.C., Bellon, H., Pérez-Segura, E., Aguillón-Robles, A., Carreño, A.-L., Bourgois, J., Cotten, J., and Benoit, M., 2008, Petrologic diversity of plio-quaternary post-subduction volcanism in Northwestern Mexico: An example from Isla San Esteban, Gulf of California, *Bulletin De La Société Géologique De France*, v. 179, no. (3–4), p. 465–481. [10.1130/B26166.1](#)
- Cande, S.C., and Leslie, R.B., 1986, Late Cenozoic Tectonics of the Southern Chile Trench, *Journal of Geophysical Research*, v. 91, no. (B1), p. 471–496. [10.1029/JB091iB01p00471](#)
- Cande, S.C., Leslie, R.B., Parra, J.C., and Hobart, M., 1987, Interaction between the Chile Ridge and Chile Trench: Geophysical and geothermal evidence, *Journal of Geophysical Research*, v. 92, no. (B1), p. 495–520. [10.1029/JB092iB01p00495](#)
- Castillo, P.R., 2008, Origin of the adakite–high-Nb basalt association and its implications for postsubduction magmatism in Baja California, Mexico, *Geological Society of America Bulletin*, v. 120, no. (3–4), p. 451–462. [10.1130/B26166.1](#)
- Castillo, P.R., 2012, Adakite petrogenesis, *Lithos*, v. 134, p. 304–316. [10.1016/j.lithos.2011.09.013](#)
- Chiaradia, M., Muntener, O., Beate, B., and Fontignie, D., 2009, Adakite-like volcanism of Ecuador: Lower crust magmatic evolution and recycling, *Contributions to Mineralogy and Petrology*, v. 158, no. (5), p. 563–588. [10.1007/s00410-009-0397-2](#)
- Cloos, M., Sapiie, B., van Ufford, Q., Weiland, A., Warren, R.J., McMahon, P.Q., Cloos, T.P., Sapiie, M., van Ufford, B., Weiland, A.Q., Warren, R.J., Q, P., and McMahon, T.P., 2005, Collisional delamination in New Guinea: The geotectonics of subducting slab breakoff, Boulder, Colorado, *Geological Society of America*.
- Cole, R.B., and Basu, A.R., 1995, Nd-Sr isotopic geochemistry and tectonics of ridge subduction and middle Cenozoic volcanism in western California, *Geological Society of America Bulletin*, v. 107, no. (2), p. 167–179. [10.1130/0016-7606\(1995\)107<0167:NSIGAT>2.3.CO;2](#)
- Cole, R.B., and Stewart, B.W., 2009, Continental margin volcanism at sites of spreading ridge subduction: Examples from Southern Alaska and Western California, *Tectonophysics*, v. 464, no. (1–4), p. 118–136. [10.1016/j.tecto.2007.12.005](#)
- Coleman, D.S., and Walker, J.D., 1990, Geochemistry of Mio-Pliocene volcanic rocks from around Panamint Valley, Death Valley area, California, in Wernicke, B.P., ed., *Basin and range extensional tectonics near the latitude of Las Vegas, Nevada*, *Geological Society of America Memoir*, p. 391–412. [10.1130/MEM176-p391](#)
- Coombs, M.L., Larsen, J.F., and Neal, C.A., 2018, Postglacial eruptive history and geochemistry of Semisopochnoi volcano, Western Aleutian Islands, Alaska (U.S. Geological Survey Scientific Investigations Report 2017–5150): Reston, US Geological Survey. [10.3133/sir20175150](#)
- Cousens, B.L., and Bevier, M.L., 1995, Discerning asthenospheric, Lithospheric, and Crustal Influences on the Geochemistry of Quaternary Basalts from the Iskut-Unuk Rivers Area, Northwestern British Columbia, *Canadian Journal of Earth Sciences*, v. 32, no. (9), p. 1451–1461. [10.1139/e95-117](#)
- Coutand, I., Diraison, M., Cobbold, P.R., Gapais, D., Rossello, E.A., and Miller, M., 1999, Structure and kinematics of a foothills transect, Lago Viedma, Southern Andes (49°30'S), *Journal of South American Earth Sciences*, v. 12, no. (1), p. 1–15. [10.1016/S0895-9811\(99\)00002-4](#)
- D'Orazio, M., Agostini, S., Innocenti, F., Haller, M.J., Manetti, P., and Mazzarini, F., 2001, Slab window-related magmatism from southernmost South America: The Late Miocene mafic volcanics from the Estancia Glencross Area (□52°S, Argentina–Chile), *Lithos*, v. 57, no. (2–3), p. 67–89. [10.1016/S0024-4937\(01\)00040-8](#)
- D'Orazio, M., Agostini, S., Mazzarini, F., Innocenti, F., Manetti, P., Haller, M.J., and Lahsen, A., 2000, The Pali Aike Volcanic Field, Patagonia: Slab-window Magmatism near the Tip of South America, *Tectonophysics*, v. 321, no. (4), p. 407–427. [10.1016/S0040-1951\(00\)00082-2](#)
- D'Orazio, M., Innocenti, F., Manetti, P., Tamponi, M., Tonarini, S., González-Ferrán, O., Lahsen, A., and Omarini, R., 2003, The Quaternary calc-alkaline volcanism of the Patagonian Andes close to the Chile triple junction: Geochemistry and petrogenesis of volcanic rocks from the Cay and Maca volcanoes (□45°S, Chile), *Journal of South American Earth Sciences*, v. 16, no. (4), p. 219–242. [10.1016/S0895-9811\(03\)00063-4](#)
- Davies, J.H., and von Blanckenburg, F., 1995, Slab breakoff: A model of lithosphere detachment and its test in the magmatism and deformation of collisional orogens, *Earth and Planetary Science Letters*, v. 129, no. (1–4), p. 85–102. [10.1016/0012-821X\(94\)00237-S](#)
- Day, J., Koppers, A.A.P., Mendenhall, B.C., and Oller, B., 2019, The 'Scripps Dike' and its implications for mid-Miocene volcanism and tectonics of the California Continental Borderland, *Journal of Sedimentary Research*, v. 17, no. (1), p. 43–55. [10.2110/sepmssp.110.02](#)
- de Lépinay, M.M., Loncke, L., Basile, C., Roest, W.R., Patriat, M., Maillard, A., and De Clarens, P., 2016, Transform continental margins–Part 2: A worldwide review, *Tectonophysics*, v. 693, p. 96–115. [10.1016/j.tecto.2016.05.038](#)
- Defant, M.J., and Drummond, M.S., 1990, Derivation of some modern arc magmas by melting of young subducted lithosphere, *Nature*, v. 347, p. 662–665. [10.1038/347662a0](#)
- Dempsey, S., 2013, *Geochemistry of volcanic rocks from the Sunda Arc* [Doctoral theses]: Durham, Durham University.
- Di Luccio, F., Persaud, P., and Clayton, R.W., 2014, Seismic structure beneath the Gulf of California: A contribution from group velocity measurements, *Geophysical Journal International*, v. 199, no. (3), p. 1861–1877. [10.1093/gji/ggu338](#)
- Dickinson, W.R., 1997, Tectonic implications of Cenozoic volcanism in coastal California, *Geological Society of America Bulletin*, v. 109, no. (8), p. 936–954. [10.1130/0016-7606\(1997\)109<0936:OTIOCV>2.3.CO;2](#)
- Dickinson, W.R., 2002, The basin and range province as a composite extensional domain, *International Geology Review*, v. 44, no. (1), p. 1–38. [10.2747/0020-6814.44.1.1](#)



- Dickinson, W.R., and Snyder, W.S., 1979a, Geometry of Subducted Slabs Related to San Andreas Transform, The Journal of Geology, v. 87, no. (6), p. 609–627. 10.1086/628456
- Dickinson, W.R., and Snyder, W.S., 1979b, Geometry of triple junctions related to San Andreas transform, Journal of Geophysical Research: Solid Earth, v. 84, no. (B2), p. 561–572. 10.1029/JB084iB02p00561
- Dostal, J., Church, B.N., Reynolds, P.H., and Hopkinson, L., 2001, Eocene volcanism in the Buck Creek basin, central British Columbia (Canada): Transition from arc to extensional volcanism, Journal of Volcanology and Geothermal Research, v. 107, no. (1–3), p. 149–170. 10.1016/S0377-0273(00)00261-4
- Eagles, G., and Jokat, W., 2014, Tectonic reconstructions for paleobathymetry in Drake Passage, Tectonophysics, v. 611, p. 28–50. 10.1016/j.tecto.2013.11.021
- Eby, G.N., 1992, Chemical subdivision of the A-type granitoids: Petrogenetic and tectonic implications, Geology, v. 20, no. (7), p. 641–644. 10.1130/0091-7613(1992)020<0641:CSOTAT>2.3.CO;2
- Edwards, B.R., and Russell, J.K., 2000, Distribution, nature, and origin of Neogene-Quaternary magmatism in the Northern Cordilleran volcanic province, Canada, Geological Society of America Bulletin, v. 112, no. (8), p. 1280–1295. 10.1130/0016-7606
- Encinas, A., Folguera, A., Rizzo, R., Molina, P., Fernández Paz, L., Litvak, V.D., Colwyn, D.A., Valencia, V.A., and Carrasco, M., 2019, Cenozoic basin evolution of the Central Patagonian Andes: Evidence from geochronology, stratigraphy, and geochemistry, Geoscience Frontiers, v. 10, no. (3), p. 1139–1165. 10.1016/j.gsf.2018.07.004
- Engebretson, D.C., Cox, A., and Gordon, R.G., 1985, Relative motions between oceanic and continental plates in the Pacific basin, Geological Society of America, Special Papers, v. 206, p. 1–59. 10.1130/SPE206-p1
- Espinoza, F., Morata, D., Pelletier, E., Maury, R.C., Suárez, M., Lagabriele, Y., Polvé, M., Bellon, H., Cotten, J., De la Cruz, R., and Guivel, C., 2005, Petrogenesis of the Eocene and Mio–Pliocene alkaline basaltic magmatism in Meseta Chile Chico, Southern Patagonia, Chile: Evidence for the participation of two slab windows, Lithos, v. 82, no. (3–4), p. 315–343. 10.1016/j.lithos.2004.09.024
- Espinoza, F., Morata, D., Polvé, M., Lagabriele, Y., Maury, R.C., de la Rupelle, A., Cotton, G.C., Bellon, H., J., and Suárez, M., 2010, Middle Miocene calc-alkaline volcanism in Central Patagonia (47°S): Petrogenesis and implications for slab dynamics, Andean Geology, v. 37, no. (2), p. 300–328. 10.5027/andgeo2010-678
- Eyuboglu, Y., 2013, Slab window magmatism and convergent margin tectonics, Geoscience Frontiers, v. 4, no. (4), p. 349–351. 10.1016/j.gsf.2013.02.002
- Farmer, G.L., Glazner, A.F., Wilshire, H.G., Wooden, J.L., Pickthorn, W.J., and Katz, M., 1995, Origin of late Cenozoic basalts at the Cima volcanic field, Mojave Desert, California, Journal of Geophysical Research: Solid Earth, v. 100, no. (B5), p. 8399–8415. 10.1029/95JB00070
- Ferrari, L., 2004, Slab detachment control on mafic volcanic pulse and mantle heterogeneity in central Mexico, Geology, v. 32, no. (1), p. 77–80. 10.1130/G19887.1
- Forsythe, R., and Nelson, E., 1985, Geological manifestations of ridge collision: Evidence from the Golfo de Penas-Taitao Basin, Southern Chile, Tectonics, v. 4, no. (5), p. 477–495. 10.1029/TC004i005p00477
- Forsythe, R.D., Nelson, E.P., Carr, M.J., Kaeding, M.E., Herve, M., Mpodozis, C., Soffia, J.M., and Harambour, S., 1986, Pliocene near-trench magmatism in southern Chile: A possible manifestation of ridge collision, Geology, v. 14, no. (1), p. 23–27. 10.1130/0091-7613(1986)14<23:PNMISC>2.0.CO;2
- Friedman, E., Polat, A., Thorkelson, D.J., and Frei, R., 2016, Lithospheric mantle xenoliths sampled by melts from upwelling asthenosphere: The Quaternary Tasse alkaline basalts of southeastern British Columbia, Canada, Gondwana Research, v. 33, p. 209–230. 10.1016/j.gr.2015.11.005
- Frost, B.R., Barnes, C.G., Collins, W.J., Arculus, R.J., Ellis, D.J., and Frost, C.D., 2001, A geochemical classification for granitic rocks, Journal of Petrology, v. 42, no. (11), p. 1771–1802. 10.1093/petrology/42.11.2033
- Gao, Y., Hou, Z., Kamber, B.S., Wei, R., Meng, X., and Zhao, R., 2007, Adakite-like porphyries from the Southern Tibetan continental collision zones: Evidence for slab melt metasomatism, Contributions to Mineralogy and Petrology, v. 153, no. (1), p. 105–120. 10.1007/s00410-006-0137-9
- Garzanti, E., Radeff, G., and Malusà, M.G., 2018, Slab breakoff: A critical appraisal of a geological theory as applied in space and time, Earth-Science Reviews, v. 177, p. 303–319. 10.1016/j.earscirev.2017.11.012
- Gastil, G., Krummenacher, D., and Minch, J., 1979, The record of Cenozoic volcanism around the Gulf of California, Geological Society of America Bulletin, v. 90, no. (9), p. 839–857. 10.1130/0016-7606(1979)90<839:TROCV>2.0.CO;2
- Georgieva, V., Gallagher, K., Sobczyk, A., Sobel, E.R., Schildgen, T.F., Ehlers, T.A., and Strecker, M.R., 2019, Effects of slab-window, alkaline volcanism, and glaciation on thermochronometer cooling histories, Patagonian Andes, Earth and Planetary Science Letters, v. 511, p. 164–176. 10.1016/j.epsl.2019.01.030
- Gill, J.B., 1981, Orogenic Andesites and Plate Tectonics, New York, Springer-Verlag. 390pp.
- Gill, J.B., Morris, J.D., and Johnson, R.W., 1993, Timescale for producing the geochemical signature of island arc magmas: U-Th-Po and Be-B systematics in recent Papua New Guinea lavas, Geochimica et Cosmochimica Acta, v. 57, no. (17), p. 4269–4283. 10.1016/0016-7037(93)90322-N
- Goddard, A.L.S., and Fosdick, J.C., 2019, Multichronometer thermochronologic modeling of migrating spreading ridge subduction in Southern Patagonia, Geology, v. 47, no. (10), p. 555–558. 10.1130/G46788Y.1
- Gorring, M., Singer, B., Gowers, J., and Kay, S.M., 2003, Plio–Pleistocene basalts from the Meseta del Lago Buenos Aires, Argentina: Evidence for asthenosphere–lithosphere interactions during slab window magmatism, Chemical Geology, v. 193, no. (3–4), p. 215–235. 10.1016/S0009-2541(02)00249-8
- Gorring, M.L., and Kay, S.M., 2001, Mantle processes and sources of Neogene slab window magmas from Southern Patagonia, Argentina, Journal of Petrology, v. 42, no. (6), p. 1067–1094. 10.1093/petrology/42.6.1067
- Gorring, M.L., Kay, S.M., Zeitler, P.K., Ramos, V.A., Rubiolo, D., Fernandez, M.I., and Panza, J.L., 1997, Neogene Patagonian plateau lavas: Continental magmas associated with ridge collision at the Chile Triple Junction, Tectonics, v. 16, no. (1), p. 1–17. 10.1029/96TC03368



- Grebennikov, A.V., 2014, A-type granites and related rocks: Petrogenesis and classification, *Russian Geology and Geophysics*, v. 55, no. (9), p. 1074–1086. [10.1016/j.rgg.2014.08.003](https://doi.org/10.1016/j.rgg.2014.08.003)
- Grebennikov, A.V., Khanchuk, A.I., Gonevchuk, V.G., and Kovalenko, S.V., 2016, Cretaceous and paleogene granitoid suites of the Sikhote-Alin area (Far East Russia): Geochemistry and tectonic implications, *Lithos*, v. 261, p. 250–261. [10.1016/j.lithos.2015.12.020](https://doi.org/10.1016/j.lithos.2015.12.020)
- Grebennikov, A.V., Popov, V.K., and Khanchuk, A.I., 2013, Experience of petrochemical typification of acid volcanic rocks from different geodynamic settings, *Russian Journal of Pacific Geology*, v. 7, no. (3), p. 212–216. [10.1134/S1819714013030044](https://doi.org/10.1134/S1819714013030044)
- Grib, E., Leonov, V., and Perepelov, A., 2009, The Karymskii volcanic center: Volcanic rock geochemistry, *Journal of Volcanology and Seismology*, v. 3, no. (6), p. 367–387. [10.1134/S0742046309060013](https://doi.org/10.1134/S0742046309060013)
- Groome, W.G., Thorkelson, D.J., Friedman, R.M., Mortensen, J.K., Massey, N.W.D., Marshall, D.D., Layer, P.W., Sisson, V.B., Roeske, S.M., and Pavlis, T.L., 2003, Magmatic and tectonic history of the Leech River Complex, Vancouver Island, British Columbia: Evidence for ridge-trench intersection and accretion of the Crescent Terrane, *in* Sisson, V.B., Roeske, S.M., and Pavlis, T.L., eds., *Geology of a transpressional orogen developed during ridge-trench interaction along the North Pacific margin*: Boulder, Colorado, Geological Society of America, p. 327–353.
- Groome, W.G., and Thorkelson, D.J., 2009, The three-dimensional thermo-mechanical signature of ridge subduction and slab window migration, *Tectonophysics*, v. 464, no. (1–4), p. 70–83. [10.1016/j.tecto.2008.07.003](https://doi.org/10.1016/j.tecto.2008.07.003)
- Grib, E., 2015, The Bol'shoi Semyachik volcanic massif, Kamchatka: Composition of the rocks and minerals, and petrogenesis, *Journal of Volcanology and Seismology*, v. 9, p. 81–103. [10.1134/S0742046315020037](https://doi.org/10.1134/S0742046315020037)
- Grove, T.L., Elkins-Tanton, L.T., Parman, S.W., Chatterjee, N., Muntener, O., and Gaetani, G.A., 2003, Fractional crystallization and mantle-melting controls on calc-alkaline differentiation trends, *Contributions to Mineralogy and Petrology*, v. 145, p. 515–533. [10.1007/s00410-003-0448-z](https://doi.org/10.1007/s00410-003-0448-z)
- Guenther, W.R., Jr, B., Reiners, D.L., P., W., and Thomson, S.N., 2010, Slab window migration and terrane accretion preserved by low-temperature thermochronology of a magmatic arc, Northern Antarctic Peninsula, *Geochemistry, Geophysics, Geosystems*, v. 11, no. (3), p. Q03001. [10.1029/2009GC002765](https://doi.org/10.1029/2009GC002765)
- Guillaume, B., Gautheron, C., Simon-Labric, T., Martinod, J., Roddaz, M., and Douville, E., 2013, Dynamic topography control on Patagonian relief evolution as inferred from low temperature thermochronology, *Earth and Planetary Science Letters*, v. 364, p. 157–167. [10.1016/j.epsl.2012.12.036](https://doi.org/10.1016/j.epsl.2012.12.036)
- Guivel, C., Lagabriele, Y., Bourgois, J., Martin, H., Arnaud, N., Fourcade, S., Cotten, J., and Maury, R.C., 2003, Very shallow melting of oceanic crust during spreading ridge subduction: Origin of near-trench quaternary volcanism at the Chile triple junction, *Journal of Geophysical Research: Solid Earth*, v. 108, no. (B7), p. 2345. [10.1029/2002JB002119](https://doi.org/10.1029/2002JB002119)
- Guivel, C., Lagabriele, Y., Bourgois, J., Maury, R., Fourcade, S., Martin, H., and Arnaud, N., 1999, New geochemical constraints for the origin of ridge-subduction-related plutonic and volcanic suites from the Chile triple junction (Taitao Peninsula and site 862, LEG ODP141 on the Taitao Ridge), *Tectonophysics*, v. 311, no. (1–4), p. 83–111. [10.1016/S0040-1951\(99\)00160-2](https://doi.org/10.1016/S0040-1951(99)00160-2)
- Guivel, C., Morata, D., Pelleter, E., Espinoza, F., Maury, R.C., Lagabriele, Y., Polvé, M., Bellon, H., Cotten, J., Benoit, M., Suárez, M., and de la Cruz, R., 2006, Miocene to late quaternary Patagonian basalts (46–47°S): Geochronometric and geochemical evidence for slab tearing due to active spreading ridge subduction, *Journal of Volcanology and Geothermal Research*, v. 149, no. (3–4), p. 346–370. [10.1016/j.jvolgeores.2005.09.002](https://doi.org/10.1016/j.jvolgeores.2005.09.002)
- Haeussler, P.J., Bradley, D., Goldfarb, R., Snee, L., and Taylor, C., 1995, Link between ridge subduction and gold mineralization in southern Alaska, *Geology*, v. 23, no. (11), p. 995–998. [10.1130/0091-7613\(1995\)023<0995:LBR5AG>2.3.CO;2](https://doi.org/10.1130/0091-7613(1995)023<0995:LBR5AG>2.3.CO;2)
- Haeussler, P.J., Bradley, D.C., Wells, R.E., and Miller, M.L., 2003, Life and death of the resurrection plate: Evidence for its existence and subduction in the Northeastern Pacific in Paleocene–Eocene time, *Geological Society of America Bulletin*, v. 115, no. (7), p. 867–880. [10.1130/0016-7606-\(2003\)115<0867:LADOTR>2.0.CO;2](https://doi.org/10.1130/0016-7606-(2003)115<0867:LADOTR>2.0.CO;2)
- Hall, R., and Spakman, W., 2015, Mantle structure and tectonic history of SE Asia, *Tectonophysics*, v. 658, p. 14–45. [10.1016/j.tecto.2015.07.003](https://doi.org/10.1016/j.tecto.2015.07.003)
- Hamilton, P.J., Johnson, R.W., Mackenzie, D.E., and O'Nions, R.K., 1983, Pleistocene volcanic rocks from the Fly-Highlands province of Western Papua New Guinea: A note on new Sr and Nd isotopic data and their petrogenetic implications, *Journal of Volcanology and Geothermal Research*, v. 18, no. (1–4), p. 449–459. [10.1016/0377-0273\(83\)90020-3](https://doi.org/10.1016/0377-0273(83)90020-3)
- Hamilton, T.S., and Dostal, J., 2001, Melting of heterogeneous mantle in a slab window environment: Examples from the middle Tertiary Masset basalts, Queen Charlotte Islands, British Columbia, *Canadian Journal of Earth Sciences*, v. 38, no. (5), p. 825–838. [10.1139/e00-095](https://doi.org/10.1139/e00-095)
- Hayes, G.P., Wald, D.J., and Johnson, R.L., 2012, Slab1.0: A three-dimensional model of global subduction zone geometries, *Journal of Geophysical Research: Solid Earth*, v. 117. [10.1029/2011jb008524](https://doi.org/10.1029/2011jb008524)
- Hekinian, R., Mühe, R., Worthington, T.J., and Stoffers, P., 2008, Geology of a submarine volcanic caldera in the Tonga Arc: Dive results, *Journal of Volcanology and Geothermal Research*, v. 176, no. (4), p. 571–582. [10.1016/j.jvolgeores.2008.05.007](https://doi.org/10.1016/j.jvolgeores.2008.05.007)
- Henry, C.D., and Aranda-Gomez, J.J., 2000, Plate interactions control middle–late Miocene, proto-Gulf and Basin and Range extension in the Southern Basin and range, *Tectonophysics*, v. 318, no. (1–4), p. 1–26. [10.1016/S0040-1951\(99\)00304-2](https://doi.org/10.1016/S0040-1951(99)00304-2)
- Hickey-Vargas, R., Holbik, S., Tormey, D., Frey, F.A., and Roa, H. M., 2016, Basaltic rocks from the Andean Southern volcanic zone: Insights from the comparison of along-strike and small-scale geochemical variations and their sources, *Lithos*, v. 258–259, p. 115–132. [10.1016/j.lithos.2016.04.014](https://doi.org/10.1016/j.lithos.2016.04.014)
- Hildebrand, R.S., and Whalen, J.B., 2017, The tectonic setting and origin of Cretaceous Batholiths within the North American Cordillera: The case for slab failure magmatism and its significance for crustal growth, Boulder, Colorado, Geological Society of America.
- Hill, K.C., and Hall, R., 2003, Mesozoic–Cenozoic evolution of Australia's New Guinea margin in a West Pacific context, *in* Hillis, R.R., and Müller, R.D., eds., *Evolution and dynamics of*

- the Australian Plate, Boulder, Colorado, Geological Society of America, p. 265–290.
- Hole, M., 1990, Geochemical evolution of Pliocene-recent post-subduction alkalic basalts from Seal Nunataks, Antarctic Peninsula, *Journal of Volcanology and Geothermal Research*, v. 40, no. (2), p. 149–167. [10.1016/0377-0273\(90\)90118-Y](#)
- Hole, M., and Larter, R.D., 1993, Trench-proximal volcanism following ridge crest-trench collision along the Antarctic Peninsula, *Tectonics*, v. 12, no. (4), p. 897–910. [10.1029/93TC00669](#)
- Hole, M., Rogers, G., Saunders, A., and Storey, M., 1991, Relation between alkalic volcanism and slab-window formation, *Geology*, v. 19, no. (6), p. 657–660. [10.1130/0091-7613\(1991\)019<0657:RBAVAS>2.3.CO;2](#)
- Hole, M., Saunders, A., Rogers, G., and Sykes, M., 1994, The relationship between alkaline magmatism, lithospheric extension and slab window formation along continental destructive plate margins, Geological Society, London, Special Publications, v. 81, p. 265–285. [10.1144/GSL.SP.1994.081.01.15](#)
- Holm, R.J., and Poke, B., 2018, Petrology and crustal inheritance of the Cloudy Bay Volcanics as derived from a fluvial conglomerate, Papuan Peninsula (Papua New Guinea): An example of geological inquiry in the absence of in situ outcrop, *Cogent Geoscience*, v. 4, no. (1), p. 1450198. [10.1080/23312041.2018.1450198](#)
- Holm, R.J., Spandler, C., and Richards, S.W., 2015, Continental collision, orogenesis and arc magmatism of the Miocene Maramuni arc, Papua New Guinea, *Gondwana Research*, v. 28, no. (3), p. 1117–1136. [10.1016/j.gr.2014.09.011](#)
- Holm, R.J., Tapster, S., Jelsma, H.A., Rosenbaum, G., and Mark, D. F., 2019, Tectonic evolution and copper-gold metallogenesis of the Papua New Guinea and Solomon Islands region: *Ore Geology Review*, v. 104, p. 208–226. [10.1016/j.oregeorev.2018.11.007](#)
- Housh, T., and McMahon, T.P., 2000, Ancient isotopic characteristics of Neogene potassic magmatism in Western New Guinea (Irian Jaya, Indonesia), *Lithos*, v. 50, no. (1), p. 217–239. [10.1016/S0024-4937\(99\)00043-2](#)
- Ickert, R.B., Thorkelson, D.J., Marshall, D.D., and Ullrich, T.D., 2009, Eocene adakitic volcanism in Southern British Columbia: Remelting of arc basalt above a slab window, *Tectonophysics*, v. 464, no. (1–4), p. 164–185. [10.1016/j.tecto.2007.10.007](#)
- Johnson, R.W., Jaques, A.L., Hickey, R.L., McKee, C.O., and Chappell, B.W., 1985, Manam Island, Papua New Guinea: Petrology and geochemistry of a Low-TiO<sub>2</sub> basaltic island-arc volcano, *Journal of Petrology*, v. 26, no. (2), p. 283–323. [10.1093/petrology/26.2.283](#)
- Kaeding, M., Forsythe, R.D., and Nelson, E.P., 1990, Geochemistry of the Taitao ophiolite and near-trench intrusions from the Chile margin triple junction, *Journal of South American Earth Sciences*, v. 3, no. (4), p. 161–177. [10.1016/0895-9811\(90\)90001-H](#)
- Kant, L.B., Tepper, J.H., Eddy, M.P., Bruce, K., and Nelson, B.K., 2018, Eocene basalt of Summit Creek: Slab breakoff magmatism in the central Washington Cascades, USA: *Lithosphere*, v. 10, no. (6), p. 792–805. [10.1130/L731.1](#)
- Kay, R.W., 1978, Aleutian magnesian andesites: Melts from subducted Pacific ocean crust, *Journal of Volcanology and Geothermal Research*, v. 4, no. (1–2), p. 117–132. [10.1016/0377-0273\(78\)90032-X](#)
- Kay, S.M., Kay, R.W., Brueckner, H.K., and Rubenstone, J.L., 1983, Tholeiitic Aleutian arc plutonism: The Finger Bay pluton, Adak, Alaska, *Contributions to Mineralogy and Petrology*, v. 82, p. 99–116. [10.1007/BF00371179](#)
- Kay, S.M., Ramos, V.A., and Marquez, M., 1993, Evidence in Cerro Pampa volcanic rocks for slab-melting prior to ridge-trench collision in Southern South America, *The Journal of Geology*, v. 101, no. (6), p. 703–714. [10.1086/648269](#)
- Kay, S.M., Tibbetts, A., and Jicha, B.R., 2014, The magmatic and tectonic evolution of Attu Island in the near Islands of the Aleutian arc, *Geological Society of America Abstracts with Programs*, v. 46, p. 448.
- Keenan, D.L., 2000, The geology and geochemistry of volcanic rocks in the Lava Mountains [UNLV retrospective theses and dissertations], California, Implications for Miocene development of the Garlock Fault.
- Kelemen, P.B., Yagodinski, G.M., and Scholl, D.W., 2003, Along-strike variation in the Aleutian island arc: Genesis of high Mg# andesite and implications for continental crust, in Eiler, J., ed., *Inside the subduction factory*, Washington, DC, American Geophysical Union Geophysical Monograph, p. 223–246.
- Keskin, M., 2003, Magma generation by slab steepening and breakoff beneath a subduction-accretion complex: An alternative model for collision-related volcanism in Eastern Anatolia, Turkey, *Geophysical Research Letters*, v. 30, no. (24), p. 8046. [10.1029/2003GL018019](#)
- Keskin, M., 2007, Eastern Anatolia: A hotspot in a collision zone without a mantle plume, in Foulger, G.R., and Jurdy, D.M., eds., *Plates, plumes, and planetary processes*, Boulder, Colorado, Geological Society of America Special Paper, p. 693–722. [10.1130/2007.2430\(32\)](#)
- Khanchuk, A.I., Grebennikov, A.V., and Ivanov, V.V., 2019, Albion-cenomanian orogenic belt and igneous province of Pacific Asia, *Russian Journal of Pacific Geology*, v. 13, no. (3), p. 187–219. [10.1134/S1819714019030035](#)
- Khanchuk, A.I., and Ivanov, V.V., 1999, Meso-cenozoic geodynamic settings and gold mineralization of the Russian far East, *Russian Geology and Geophysics*, v. 40, no. (11), p. 1607–1617.
- Khanchuk, A.I., Kemkin, I.V., and Kruk, N.N., 2016, The Sikhote-Alin orogenic belt, Russian South East: Terranes and the Formation of Continental Lithosphere Based on Geological and Isotopic Data, *Journal of Asian Earth Sciences*, v. 120, p. 117–138. [10.1016/j.jseae.2015.10.023](#)
- Kimura, J.-I., and Yoshida, T., 2006, Contributions of slab fluid, Mantle Wedge and Crust to the Origin of Quaternary Lavas in the NE Japan Arc, *Journal of Petrology*, v. 47, no. (11), p. 2185–2232. [10.1093/petrology/egl041](#)
- Kinoshita, O., 1999, A migration model of magmatism explaining a ridge subduction, And Its Details on a Statistical Analysis of the Granite Ages in Cretaceous Southwest Japan, *Island Arc*, v. 8, no. (2), p. 181–189. [10.1046/j.1440-1738.1999.00230.x](#)
- Kon, Y., Komiya, T., Anma, R.Y.O., Hirata, T., Shibuya, T., Yamamoto, S., and Maruyama, S., 2013, Petrogenesis of the ridge subduction-related granitoids from the Taitao Peninsula, Chile Triple Junction Area, *Geochemical Journal*, v. 47, no. (2), p. 167–183. [10.2343/geochemj.2.0251](#)
- Košler, J., Magna, T., Mlčoch, B., Mixa, P., Nývlt, D., and Holub, F., 2009, Combined Sr, Nd, Pb and Li Isotope Geochemistry of Alkaline Lavas from Northern James Ross Island (Antarctic Peninsula) and Implications for Back-arc Magma Formation,

- Chemical Geology, v. 258, no. (3-4), p. 207–218. 10.1016/j.chemgeo.2008.10.006
- Kuehn, C., Guest, B., Russell, J.K., and Benowitz, J.A., 2015, The Satah Mountain and Baldface Mountain volcanic fields: Pleistocene hot spot volcanism in the Anahim Volcanic Belt, West-central British Columbia, Canada, *Bulletin of Volcanology*, v. 77, p. 19. 10.1007/s00445-015-0907-1
- Lagabriele, Y., Bourgois, J., Dymont, J., and Pelletier, B., 2015, Lower plate deformation at the Chile triple junction from the paleomagnetic record (45°30'S–46°S), *Tectonics*, v. 34, no. (8), p. 1646–1660. 10.1002/2014TC003773
- Lagabriele, Y., Guivel, C., Maury, R.C., Bourgois, J., Fourcade, S., and Martin, H., 2000, Magmatic–tectonic effects of high thermal regime at the site of active ridge subduction: The Chile Triple Junction model, *Tectonophysics*, v. 326, no. (3–4), p. 255–268. 10.1016/S0040-1951(00)00124-4
- Lagabriele, Y., Moigne, J.L., Maury, R.C., Cotten, J., and Bourgois, J., 1994, Volcanic record of the subduction of an active spreading ridge, Taitao Peninsula (Southern Chile), *Geology*, v. 22, no. (6), p. 515–518. 10.1130/0091-7613(1994)022<0515:VROTSO>2.3.CO;2
- Leuthold, J., Müntener, O., Baumgartner, L.P., and Putlitz, B., 2014, Petrological constraints on the recycling of mafic crystal mushes and intrusion of braided sills in the Torres del Paine Mafic Complex (Patagonia), *Journal of Petrology*, v. 55, no. (5), p. 917–949. 10.1093/petrology/egu011
- Leuthold, J., Müntener, O., Baumgartner, L.P., Putlitz, B., and Chiaradia, M., 2013, A detailed geochemical study of a shallow arc-related laccolith; the Torres del Paine Mafic Complex (Patagonia), *Journal of Petrology*, v. 54, no. (2), p. 273–303. 10.1093/petrology/egs069
- Leuthold, J., Müntener, O., Baumgartner, L.P., Putlitz, B., Ovtcharova, M., and Schaltegger, U., 2012, Time resolved construction of a bimodal laccolith (Torres del Paine, Patagonia), *Earth and Planetary Science Letters*, v. 325–326, p. 85–92. 10.1016/j.epsl.2012.01.032
- Levin, V., Shapiro, N.M., Park, J., and Ritzwoller, M.H., 2005, Slab portal beneath the Western Aleutians, *Geology*, v. 33, no. (4), p. 253–256. 10.1130/G20863.1
- Liu, M., and Furlong, K.P., 1992, Cenozoic volcanism in the California Coast Ranges: Numerical solutions, *Journal of Geophysical Research*, v. 97, no. (B4), p. 4941–4951. 10.1029/92JB00193
- Lonsdale, P., 1991, Structural patterns of the Pacific floor off-shore of peninsular California, in Dauphin, J.P., and Simoneit, B.R.T., eds., *The Gulf and peninsular province of the Californias*, American Association of Petroleum Geologists, AAPG Special Volumes, Memoir, p. 87–125. 10.1306/M47542C7
- Luhr, J.F., Aranda-Gómez, J.J., and Housh, T.B., 1995, San Quintín Volcanic Field, Baja California Norte, Mexico: Geology, Petrology, and Geochemistry, *Journal of Geophysical Research: Solid Earth*, v. 100, no. (B6), p. 10353–10380. 10.1029/95JB00037
- Mackenzie, D.E., and Johnson, R.W., 1984, Pleistocene volcanoes of the Western Papua New Guinea Highlands: Morphology, geology, petrography, and modal and chemical analyses, Canberra, Australian Government Publishing Service.
- Madsen, J.K., Thorkelson, D.J., Friedman, R.M., and Marshall, D. D., 2006, Cenozoic to recent plate configurations in the Pacific Basin: Ridge subduction and slab window magmatism in Western North America, *Geosphere*, v. 2, no. (1), p. 11–34. 10.1130/GES00020.1
- Mann, P., and Taira, A., 2004, Global tectonic significance of the Solomon Islands and Ontong Java Plateau convergent zone: *Tectonophysics*, v. 389, no. (3-4), p. 137–190. 10.1016/j.tecto.2003.10.024
- Mark, C., Chew, D., and Gupta, S., 2017, Does slab-window opening cause uplift of the overriding plate? A case study from the Gulf of California, *Tectonophysics*, v. 719–720, p. 162–175. 10.1016/j.tecto.2017.02.008
- Marske, J.P., Pietruszka, A.J., Trusdell, F.A., and Garcia, M.O., 2011, Geochemistry of Southern Pagan Island lavas, Mariana Arc: The Role of Subduction Zone Processes: Contributions to Mineralogy and Petrology, v. 162, no. (2), p. 231–252. 10.1007/s00410-010-0592-1
- Martin, H., 1999, The adakitic magmas: Modern analogues of Archaean granitoids, *Lithos*, v. 46, no. (3), p. 411–429. 10.1016/S0024-4937(98)00076-0
- Martin, H., Smithies, R.H.M., Rapp, R., Moyen, J.F., and Champion, D., 2005, An overview of adakite, tonalitetrondhjemite-granodiorite (TTG) and sanukitoid: Relationships and some implications for crustal evolution, *Lithos*, v. 79, no. (1–2), p. 1–24. 10.1016/j.lithos.2004.04.048
- Martynov, A.Y., and Martynov, Y.A., 2017, Pleistocene basaltic volcanism of Kunashir Island (Kuril island arc): Mineralogy, Geochemistry, and Results of Computer Simulation, *Petrology*, v. 25, p. 206–225. 10.1134/S0869591117020035
- Martynov, Y.A., Khanchuk, A., Kimura, J.-I., Rybin, A., and Martynov, A.Y., 2010, Geochemistry and petrogenesis of volcanic rocks in the Kuril Island Arc, *Petrology*, v. 18, no. (5), p. 489–513. 10.1134/S0869591110050048
- Martynov, Y.A., Khanchuk, A.I., Grebennikov, A.V., Chashchin, A. A., and Popov, V.K., 2017, Late Mesozoic and Cenozoic volcanism of the East Sikhote-Alin area (Russian Far East): A new synthesis of geological and petrological data, *Gondwana Research*, v. 47, p. 358–371. 10.1016/j.gr.2017.01.005
- McCarthy, A., Tugend, J., Mohn, G., Candiotti, L., Chelle-Michou, C., Arculus, R., Schmalholz, S.M., and Müntener, O., 2020, A case of Ampferer-type subduction and consequences for the Alps and the Pyrenees, *American Journal of Science*, v. 320, no. (4), p. 313–372. 10.2475/04.2020.01
- McCrory, P.A., and Wilson, D.S., 2009, Introduction to special issue on: Interpreting the tectonic evolution of pacific rim margins using plate kinematics and slab-window volcanism, *Tectonophysics*, v. 464, no. (1–4), p. 3–9. 10.1016/j.tecto.2008.03.015
- McCrory, P.A., Wilson, D.S., and Stanley, R.G., 2009, Continuing evolution of the Pacific–Juan de Fuca–North America slab window system—A trench–ridge–transform example from the Pacific Rim, *Tectonophysics*, v. 464, no. (1-4), p. 30–42. 10.1016/j.tecto.2008.01.018
- McDowell, F.W., McMahon, T.P., Warren, P.Q., and Cloos, M., 1996, Pliocene Cu-Au-bearing igneous intrusions of the Gunung Bijih (Ertsberg) District, Irian Jaya, Indonesia: K-Ar Geochronology, *The Journal of Geology*, v. 104, no. (3), p. 327–340. 10.1086/629828
- McKenzie, D.P., and Morgan, W., 1969, Evolution of triple junctions, *Nature*, v. 224, p. 125–133. 10.1038/224125a0
- Michael, P.J., 1984, Chemical differentiation of the Cordillera Paine granite (southern Chile) by in situ fractional crystallization, *Contributions to Mineralogy and Petrology*, v. 87, p. 179–195. 10.1007/BF00376223

- Michael, P.J., 1991, Intrusion of basaltic magma into a crystalizing granitic magma chamber: The Cordillera del Paine pluton in Southern Chile, *Contributions to Mineralogy and Petrology*, v. 108, no. (4), p. 396–418. [10.1007/BF00303446](#)
- Michaud, F., Royer, J.Y., Bourgois, J., Dymont, J., Calmus, T., Bandy, W., Sosson, M., Mortera-Gutiérrez, C., Sichler, B., Rebolledo-Viera, M., and Pontoise, B., 2006, Oceanic-ridge subduction vs. slab break off: Plate tectonic evolution along the Baja California Sur continental margin since 15 Ma, *Geology*, v. 34, no. (1), p. 13–16. [10.1130/g22050.1](#)
- Michel, J., Baumgartner, L., Putlitz, B., Schaltegger, U., and Ovtcharova, M., 2008, Incremental growth of the Patagonian Torres del Paine laccolith over 90 k.y, *Geology*, v. 36, no. (6), p. 459–462. [10.1130/G24546A.1](#)
- Moreno, F.A., and Demant, A., 1999, The Recent Isla San Luis volcanic centre: Petrology of a rift-related volcanic suite in the northern Gulf of California, Mexico, *Journal of Volcanology and Geothermal Research*, v. 93, no. (1–2), p. 31–52. [10.1016/S0377-0273\(99\)00083-9](#)
- Müntener, O., Ewing, T., Baumgartner, L.P., Manzini, M., Roux, T., Pellaud, P., and Allemann, L., 2018, Source and fractionation controls on subduction-related plutons and dike swarms in southern Patagonia (Torres del Paine area) and the low Nb/Ta of upper crustal igneous rocks, *Contributions to Mineralogy and Petrology*, v. 173, p. 38. [10.1007/s00410-018-1467-0](#)
- Nakamura, H., and Iwamori, H., 2013, Generation of adakites in a cold subduction zone due to double subducting plates, *Contributions to Mineralogy and Petrology*, v. 165, p. 1107–1134. [10.1007/s00410-013-0850-0](#)
- Natal'in, B., 1993, History and modes of Mesozoic accretion in Southeastern Russia, *Island Arc*, v. 2, no. (1), p. 15–34. [10.1111/j.1440-1738.1993.tb00072.x](#)
- Negrete-Aranda, R., and Cañón-Tapia, E., 2008, Post-subduction volcanism in the Baja California Peninsula, Mexico: The Effects of Tectonic Reconfiguration in Volcanic Systems, *Lithos*, v. 102, no. (1–2), p. 392–414. [10.1016/j.lithos.2007.08.013](#)
- Negrete-Aranda, R., Contreras, J., and Spelz, R.M., 2013, Viscous dissipation, Slab Melting, and Post-subduction Volcanism in South-central Baja California, Mexico, *Geosphere*, v. 9, no. (6), p. 1714–1728. [10.1130/GES00901.1](#)
- Ormerod, D.S., Rogers, N.W., and Hawkesworth, C.J., 1991, Melting in the lithospheric mantle: Inverse modelling of alkali-olivine basalts from the Big Pine Volcanic Field, California, *Contributions to Mineralogy and Petrology*, v. 108, p. 305–317. [10.1007/BF00285939](#)
- Pallares, C., Maury, R.C., Bellon, H., Royer, J.-Y., Calmus, T., Aguillón-Robles, A., Cotten, J., Benoit, M., Michaud, F., and Bourgois, J., 2007, Slab-tearing following ridge-trench collision: Evidence from Miocene volcanism in Baja California, México, *Journal of Volcanology and Geothermal Research*, v. 161, no. (1–2), p. 95–117. [10.1016/j.jvolgeores.2006.11.002](#)
- Patchett, P.J., and Chase, C.G., 2002, Role of transform continental margins in major crustal growth episodes, *Geology*, v. 30, no. (1), p. 39–42. [10.1130/0091-7613\(2002\)030<0039:ROTCMI>2.0.CO;2](#)
- Pearce, J.A., 1996, Sources and settings of granitic rocks, *Episodes*, v. 19, no. (4), p. 120–125. [10.18814/epiugs/1996/v19i4/005](#)
- Pearce, J.A., 2008, Geochemical fingerprinting of oceanic basalts with applications to ophiolite classification and the search for Archean oceanic crust, *Lithos*, v. 100, no. (1–4), p. 14–48. [10.1016/j.lithos.2007.06.016](#)
- Pearce, J.A., 2014, Immobile element fingerprinting of ophiolites, *Elements*, v. 10, no. (2), p. 101–108. [10.2113/gselements.10.2.101](#)
- Pearce, J.A., and Robinson, P.T., 2010, The Troodos ophiolitic complex probably formed in a subduction initiation, *Slab Edge Setting*, *Gondwana Research*, v. 18, no. (1), p. 60–81. [10.1016/j.gr.2009.12.003](#)
- Pearce, J.A., Stern, R.J., Bloomer, S.H., and Fryer, P., 2005, Geochemical mapping of the Mariana arc-basin system: Implications for the nature and distribution of subduction components, *Geochemistry, Geophysics, Geosystems*, v. 6, no. (7), p. Q07006. [10.1029/2004GC000895](#)
- Petricca, P., and Carminati, E., 2016, Present-day stress field in subduction zones: Insights from 3D viscoelastic models and data, *Tectonophysics*, v. 667, p. 48–62. [10.1016/j.tecto.2015.11.010](#)
- Polonia, A., Torelli, L., Brancolini, G., and Loreto, M.F., 2007, Tectonic accretion versus erosion along the southern Chile trench: Oblique subduction and margin segmentation, *Tectonics*, v. 26, no. (3), p. Tc3005. [10.1029/2006TC001983](#)
- Pubellier, M., and Ego, F., 2002, Anatomy of an escape tectonic zone: Western Irian Jaya (Indonesia), *Tectonics*, v. 21, no. (4), p. 1–1–16. [10.1029/2001TC901038](#)
- Ramos, V.A., 2005, Seismic ridge subduction and topography: Foreland deformation in the Patagonian Andes, *Tectonophysics*, v. 399, no. (1–4), p. 73–86. [10.1016/j.tecto.2004.12.016](#)
- Ramos, V.A., 2009, Anatomy and global context of the Andes: Main geologic features and the Andean orogenic cycle, in Kay, S.M., Ramos, V.A., and Dickinson, W.R., eds., *Backbone of the Americas: Shallow subduction, plateau uplift, and ridge and terrane collision*, Washington, DC, Geological Society of America, p. 31–65.
- Ramos, V.A., and Kay, S.M., 1992, Southern Patagonian plateau basalts and deformation: Back arc testimony of ridge collisions, *Tectonophysics*, v. 205, no. (1–3), p. 261–282. [10.1016/0040-1951\(92\)90430-E](#)
- Ramos, V.A., Kay, S.M., and Singer, B.S., 2004, Las adakitas de la cordillera Patagónica: Nuevas evidencias geoquímicas y geocronológicas, *Revista de la Asociación Geológica Argentina*, v. 59, p. 693–706
- Richards, J.P., 1990, Petrology and geochemistry of alkalic intrusives at the Porgera gold deposit, Papua New Guinea, *Journal of Geochemical Exploration*, v. 35, no. (1–3), p. 141–199. [10.1016/0375-6742\(90\)90038-C](#)
- Richards, J.P., and Ledlie, I., 1993, Alkalic intrusive rocks associated with the Mount Kare gold deposit, Papua New Guinea; Comparison with the Porgera Intrusive Complex, *Economic Geology*, v. 88, no. (4), p. 755–781. [10.2113/gsecongeo.88.4.755](#)
- Robinson, F.A., Bonin, B., Pease, V., and Anderson, J., 2017, A discussion on the tectonic implications of Ediacaran late-to post-orogenic A-type granite in the northeastern Arabian Shield, Saudi Arabia, *Tectonics*, v. 36, no. (3), p. 582–600. [10.1002/2016TC004320](#)
- Rogers, N.W., Hawkesworth, C.J., and Ormerod, D.S., 1995, Late Cenozoic basaltic magmatism in the Western Great Basin, California and Nevada: *Journal of Geophysical Research: Solid Earth*, v. 100, no. (B6), p. 10287–10301. [10.1029/94JB02738](#)



- Rossetti, F., Nasrabad, M., Theye, T., Gerdes, A., Monié, P., Lucci, F., and Vignaroli, G., 2014, Adakite differentiation and emplacement in a subduction channel: The late Paleocene Sabzevar magmatism (NE Iran), *GSA Bulletin*, **10.1130/B30913.1**, 3–4.
- Sahagian, D., Proussevitch, A., and Carlson, W., 2002, Timing of Colorado plateau uplift: Initial constraints from vesicular basalt-derived paleoelevations, *Geology*, v. 30, no. (9), p. 807–810. [10.1130/0091-7613\(2002\)030<0807:TOCPUI>2.0.CO;2](https://doi.org/10.1130/0091-7613(2002)030<0807:TOCPUI>2.0.CO;2)
- Santibáñez, I., Cembrano, J., García-Pérez, T., Costa, C., Yáñez, G., Marquardt, C., Arancibia, G., and González, G., 2019, Crustal faults in the Chilean Andes: Geological constraints and seismic potential, *Andean Geology*, v. 46, no. (1), p. 32–65. [10.5027/andgeoV46n1-3067](https://doi.org/10.5027/andgeoV46n1-3067)
- Saunders, A., Rogers, G., Marriner, G., Terrell, D., and Verma, S., 1987, Geochemistry of Cenozoic volcanic rocks, Baja California, Mexico: Implications for the Petrogenesis of Post-subduction Magmas, *Journal of Volcanology and Geothermal Research*, v. 32, no. (1-3), p. 223–245. [10.1016/0377-0273\(87\)90046-1](https://doi.org/10.1016/0377-0273(87)90046-1)
- Savov, I.P., Leeman, W.P., Lee, C.-T.A., and Shirey, S.B., 2009, Boron isotopic variations in NW USA rhyolites: Yellowstone, Snake River Plain, Eastern Oregon, *Journal of Volcanology and Geothermal Research*, v. 188, no. (1-3), p. 162–172. [10.1016/j.jvolgeores.2009.03.008](https://doi.org/10.1016/j.jvolgeores.2009.03.008)
- Scalabrino, B., Lagabrielle, Y., Malavielle, J., Dominguez, S., Melnick, D., Espinoza, F., Suarez, M., and Rossello, E., 2010, A morphotectonic analysis of central Patagonian Cordillera: Negative inversion of the Andean belt over a buried spreading center?, *Tectonics*, v. 29, no. (2), p. TC2010. [10.1029/2009TC002453](https://doi.org/10.1029/2009TC002453)
- Schellart, W.P., and Rawlinson, N., 2013, Global correlations between maximum magnitudes of subduction zone interface thrust earthquakes and physical parameters of subduction zones, *Physics of the Earth and Planetary Interiors*, v. 225, p. 41–67. [10.1016/j.pepi.2013.10.001](https://doi.org/10.1016/j.pepi.2013.10.001)
- Schmitt, A.K., Romer, R.L., and Stimac, J.A., 2006, Geochemistry of volcanic rocks from the Geysers geothermal area, California Coast Ranges, *Lithos*, v. 87, no. (1-2), p. 80–103. [10.1016/j.lithos.2005.05.005](https://doi.org/10.1016/j.lithos.2005.05.005)
- Seitz, S., Putlitz, B., Baumgartner, L.P., and Bouvier, A.-S., 2018, The role of crustal melting in the formation of rhyolites: Constraints from SIMS oxygen isotope data (Chon Aike Province, Patagonia, Argentina), *American Mineralogist*, v. 103, no. (12), p. 1027–2011. [10.2138/am-2018-6520](https://doi.org/10.2138/am-2018-6520)
- Sengör, A.C., and Natal'in, B.A., 1996, Turke-type orogeny and its role in the making of the continental crust, *Annual Review of Earth and Planetary Sciences*, v. 24, p. 263–337. [10.1146/annurev.earth.24.1.263](https://doi.org/10.1146/annurev.earth.24.1.263)
- Severinghaus, J., and Atwater, T., 1990, Cenozoic geometry and thermal state of the subducting slabs beneath western North America, in Wernicke, B.P., ed., *Basin and range extensional tectonics near the latitude of Las Vegas, Nevada, CO*, Geological Society of America Memoir, p. 1–22.
- Sharma, M., Basu, A.R., Cole, R.B., and DeCelles, P.G., 1991, Basalt-rhyolite volcanism by MORB-continental crust interaction: Nd, Sr-isotopic and Geochemical Evidence from Southern San Joaquin Basin, California, *Contributions to Mineralogy and Petrology*, v. 109, p. 159–172. [10.1007/BF00306476](https://doi.org/10.1007/BF00306476)
- Shen, X.-M., Zhang, H.-X., Wang, Q., Ma, L., and Yang, Y.-H., 2014, Early silurian (~ 440 Ma) adakitic, andesitic and Nb-enriched basaltic lavas in the southern Altay Range, Northern Xinjiang (Western China): Slab melting and implications for crustal growth in the Central Asian Orogenic Belt, *Lithos*, v. 206–207, p. 234–251. [10.1016/j.lithos.2014.07.024](https://doi.org/10.1016/j.lithos.2014.07.024)
- Shuto, K., Nohara-Imanaka, R., Sato, M., Takahashi, T., Takazawa, E., Kawabata, H., Takanashi, K., Ban, M., Watanabe, N., and Fujibayashi, N., 2015, Across-arc variations in geochemistry of Oligocene to quaternary basalts from the NE Japan arc: Constraints on source composition, Mantle Melting and Slab Input Composition, *Journal of Petrology*, v. 56, no. (11), p. 2257–2297. [10.1093/petrology/egv073](https://doi.org/10.1093/petrology/egv073)
- Smith, D.R., and Leeman, W.P., 1987, Petrogenesis of Mount St. Helens Dacitic Magmas: *Journal of Geophysical Research: Solid Earth*, v. 92, no. B10, p. 10313–10334. [10.1029/JB092iB10p10313](https://doi.org/10.1029/JB092iB10p10313)
- Smith, E.I., Sanchez, A., Keenan, D.L., and Monastero, F.C., 2002, Stratigraphy and geochemistry of volcanic rocks in the Lava Mountains, California: Implications for the Miocene development of the Garlock fault, in Glazner, A.F., Walker, J.D., and Bartley, J.M., eds., *Geologic evolution of the Mojave desert and southwestern basin and range*, Boulder, Colorado, Geological Society of America Memoir, p. 151–160.
- Solari, M., Hervé, F., Martinod, J., Le Roux, J., Ramírez, L., and Palacios, C., 2008, Geotectonic evolution of the Bransfield Basin, Antarctic Peninsula: Insights from Analogue Models, *Antarctic Science*, v. 20, no. (2), p. 185–196. [10.1017/S095410200800093X](https://doi.org/10.1017/S095410200800093X)
- Stern, C.R., 2004, Active Andean volcanism: Its geologic and tectonic setting, *Revista Geológica De Chile*, v. 31, no. (2), p. 161–206. [10.4067/S0716-02082004000200001](https://doi.org/10.4067/S0716-02082004000200001)
- Stern, C.R., Frey, F.A., Futa, K., Zartman, R.E., Peng, Z., and Kurtis Kyser, T., 1990, Trace-element and Sr, Nd, Pb, and O Isotopic Composition of Pliocene and Quaternary Alkali Basalts of the Patagonian Plateau Lavas of Southern Most South America, *Contributions to Mineralogy and Petrology*, v. 104, p. 294–308. [10.1007/BF00321486](https://doi.org/10.1007/BF00321486)
- Stern, C.R., and Kilian, R., 1996, Role of the subducted slab, Mantle Wedge and Continental Crust in the Generation of Adakites from the Andean Austral Volcanic Zone, *Contributions to Mineralogy and Petrology*, v. 123, p. 263–281. [10.1007/s004100050155](https://doi.org/10.1007/s004100050155)
- Stock, J.M., and Hodges, K.V., 1989, Pre-Pliocene extension around the Gulf of California and the transfer of Baja California to the Pacific Plate, *Tectonics*, v. 8, no. (1), p. 99–115. [10.1029/TC008i001p00099](https://doi.org/10.1029/TC008i001p00099)
- Sue, C., and Ghiglione, M.C., 2016, Wrenching tectonism in the Southernmost Andes and the Scotia Sea constrained from fault kinematic and seismotectonic overviews, in Ghiglione, M.C., ed., *Geodynamic evolution of the Southernmost Andes*, New York, Springer Earth System Sciences, p. 137–172.
- Sweetkind, D.S., Rytuba, J.J., Langenheim, V.E., and Fleck, R.J., 2011, Geology and geochemistry of volcanic centers within the Eastern half of the Sonoma volcanic field, Northern San Francisco Bay Region, California, *Geosphere*, v. 7, no. (3), p. 629–657. [10.1130/GES00625.1](https://doi.org/10.1130/GES00625.1)
- Tamura, Y., 2002, Remelting of an Andesitic Crust as a possible origin for rhyolitic magma in oceanic arcs: An example from the Izu-Bonin arc, *Journal of Petrology*, v. 43, no. (6), p. 1029–1047. [10.1093/petrology/43.6.1029](https://doi.org/10.1093/petrology/43.6.1029)
- Taylor, B., 2006, The single largest oceanic plateau: Ontong Java–Manihiki–Hikurangi, *Earth and Planetary Science*

- Letters, v. 241, no. (3–4), p. 372–380. [10.1016/j.epsl.2005.11.049](#)
- Ten Brink, U.S., Miller, N.C., Andrews, B.D., Brothers, D.S., and Haeussler, P.J., **2018**, Deformation of the Pacific/North America plate boundary at Queen Charlotte Fault: The possible role of rheology, *Journal of Geophysical Research: Solid Earth*, v. 123, no. (5), p. 4223–4242. [10.1002/2017JB014770](#)
- The Database GEOROC, Geochemistry of rocks of the oceans and continents. <http://georoc.mpch-mainz.gwdg.de/georoc/>.
- Thorkelson, D.J., **1996**, Subduction of diverging plates and the principles of slab window formation, *Tectonophysics*, v. 255, no. (1–2), p. 47–63. [10.1016/0040-1951\(95\)00106-9](#)
- Thorkelson, D.J., and Breitsprecher, K., **2005**, Partial melting of slab window margins: Genesis of adakitic and non-adakitic magmas, *Lithos*, v. 79, no. (1–2), p. 25–41. [10.1016/j.lithos.2004.04.049](#)
- Thorkelson, D.J., Madsen, J.K., and Slaggett, C.L., **2011**, Mantle flow through the Northern Cordilleran slab window revealed by volcanic geochemistry, *Geology*, v. 39, no. (3), p. 267–270. [10.1130/G31522.1](#)
- Thorkelson, D.J., and Taylor, R.P., **1989**, Cordilleran slab windows, *Geology*, v. 17, no. (9), p. 833–836. [10.1130/0091-7613\(1989\)017<0833:CSW>2.3.CO;2](#)
- Timm, C., Graham, I.J., de Ronde, C.E., Leybourne, M.I., and Woodhead, J., **2011**, Geochemical evolution of Monowai volcanic center: New insights into the Northern Kermadec arc subduction system, SW Pacific, *Geochemistry, Geophysics, Geosystems*, v. 12, no. (8), p. Q0AF01. [10.1029/2011GC003654](#)
- Tregoning, P., and Gorbato, A., **2004**, Evidence for active subduction at the New Guinea Trench, *Geophysical Research Letters*, v. 31, no. (13), p. L13608. [10.1029/2004GL020190](#)
- Valentine, G.A., Cortés, J.A., Widom, E., Smith, E.I., Rasoazanamparany, C., Johnsen, R., Briner, J.P., Harp, A.G., and Turrin, B., **2017**, Lunar crater volcanic field (Reveille and pancake ranges, Basin and Range Province, Nevada, USA), *Geosphere*, v. 13, no. (2), p. 391–438. [10.1130/GES01428.1](#)
- van Dongen, M., Weinberg, R.F., Tomkins, A.G., Armstrong, R.A., and Woodhead, J.D., **2010**, Recycling of Proterozoic crust in Pleistocene juvenile magma and rapid formation of the Ok Tedi porphyry Cu–Au deposit, Papua New Guinea, *Lithos*, v. 114, no. (3–4), p. 282–292. [10.1016/j.lithos.2009.09.003](#)
- Viccaro, M., Giuffrida, M., Nicotra, E., and Ozerov, A.Y., **2012**, Magma storage, ascent and recharge history prior to the 1991 eruption at Avachinsky Volcano, Kamchatka, Russia: Inferences on the plumbing system geometry, *Lithos*, v. 140–141, p. 11–24. [10.1016/j.lithos.2012.01.019](#)
- Vidal-Solano, J.R., Demant, A., Paz Moreno, F.A., Lapiere, H., Ortega-Rivera, M.A., and Lee, J.K., **2008**, Insights into the tectonomagmatic evolution of NW Mexico: Geochronology and geochemistry of the Miocene volcanic rocks from the Pinacate area, Sonora, *Geological Society of America Bulletin*, v. 120, no. (5–6), p. 691–708. [10.1130/B26053.1](#)
- Walton, M.A.L., Gulick, S.P.S., Haeussler, P.J., Roland, E.C., and Trehu, A.M., **2015**, Basement and regional structure along strike of the Queen Charlotte fault in the context of modern and historical earthquake ruptures, *Bulletin of the Seismological Society of America*, v. 105, no. (2B), p. 1090–1105. [10.1785/0120140174](#)
- Wang, Y., Forsyth, D.W., Rau, C.J., Carriero, N., Schmandt, B., Gaherty, J.B., and Savage, B., **2013**, Fossil slabs attached to unsubducted fragments of the Farallon plate, *Proceedings of the National Academy of Sciences of the United States of America*, v. 110, no. (14), p. 5342–5346. [10.1073/pnas.1214880110](#)
- Webb, M., White, L.T., Jost, B.M., Tiranda, H., and BouDagher-Fadel, M., **2020**, The history of Cenozoic magmatism and collision in NW New Guinea – New insights into the tectonic evolution of the Northernmost margin of the Australian Plate, *Gondwana Research*, v. 82, p. 12–38. [10.1016/j.gr.2019.12.010](#)
- Weigand, P.W., Savage, K.L., and Nicholson, C., **2002**, The Conejo Volcanics and other Miocene volcanic suites in Southwestern California, in Barth, A., ed., *Contributions to Crustal Evolution of the Southwestern United States*, Boulder, Colorado, Geological Society of America Special Paper, p. 187–204. [10.1130/0-8137-2365-5.187](#)
- Whalen, J.B., Currie, K.L., and Chappell, B.W., **1987**, A-type granites: Geochemical characteristics, Discrimination and Petrogenesis, *Contributions to Mineralogy and Petrology*, v. 95, p. 407–419. [10.1007/BF00402202](#)
- Whalen, J.B., and Hildebrand, R.S., **2019**, Trace element discrimination of arc, Slab Failure, and A-type Granitic Rocks, *Lithos*, v. 348–349, p. 105179. [10.1016/j.lithos.2019.105179](#)
- White, L.T., Hall, R., Gunawan, I., and Kohn, B., **2019**, Tectonic mode switches recorded at the Northern edge of the Australian Plate during the Pliocene and Pleistocene, *Tectonics*, v. 38, no. (1), p. 281–306. [10.1029/2018TC005177](#)
- Wilson, D.S., McCrory, P.A., and Stanley, R.G., **2005**, Implications of volcanism in Coastal California for the Neogene deformation history of Western North America, *Tectonics*, v. 24, no. (3), p. TC3008. [10.1029/2003TC001621](#)
- Wilson, J.T., **1965**, A new class of faults and their bearing on continental drift, *Nature*, v. 207, p. 343–347. [10.1038/207343a0](#)
- Windley, B.F., and Xiao, W., **2018**, Ridge subduction and slab windows in the Central Asian Orogenic Belt: Tectonic implications for the evolution of an accretionary orogen, *Gondwana Research*, v. 61, p. 73–87. [10.1016/j.gr.2018.05.003](#)
- Yogodzinski, G., Lees, J., Churikova, T., Dorendorf, F., Wöerner, G., and Volynets, O., **2001**, Geochemical evidence for the melting of subducting oceanic lithosphere at plate edges, *Nature*, v. 409, no. (6819), p. 500–504. [10.1038/35054039](#)
- Yogodzinski, G.M., Brown, S.T., Kelemen, P.B., Vervoort, J.D., Portnyagin, M., Sims, K.W.W., Hoernle, K., Jicha, B.R., and Werner, R., **2015**, The role of subducted basalt in the source of island arc magmas: Evidence from Seafloor Lavas of the Western Aleutians, *Journal of Petrology*, v. 56, no. (3), p. 441–492. [10.1093/petrology/egv006](#)
- Yogodzinski, G.M., Kay, R.W., Volynets, O.N., Koloskov, A.V., and Kay, S.M., **1995**, Magnesian andesite in the Western Aleutian Komandorsky region: Implications for slab melting and processes in the mantle wedge, *Geological Society of America Bulletin*, v. 107, no. (5), p. 505–519. [10.1130/0016-7606\(1995\)107<0505:MAITWA>2.3.CO;2](#)
- Zhang, J., Davidson, J.P., Humphreys, M.C.S., Macpherson, C. G., and Neill, I., **2015**, Magmatic enclaves and andesitic lavas from Mt. Lamington, Papua New Guinea: Implications for Recycling of Earlier-fractionated Minerals through Magma Recharge, *Journal of Petrology*, v. 56, no. (11), p. 2223–2256. [10.1093/petrology/egv071](#)